

INSTITUTE OF GAS TECHNOLOGY
HT CENTER
CHICAGO, ILLINOIS 60616

PREPARATION OF A
COAL CONVERSION SYSTEMS
TECHNICAL DATA BOOK

ERDA Contract No. 14-32-0001-1730
Report No. 4
February 1975

Project 8964 Status Report
for
ENERGY RESEARCH AND DEVELOPMENT ADMINISTRATION



INSTITUTE OF GAS TECHNOLOGY - IIT CENTER - CHICAGO 60616

Project Status Report
For

ENERGY RESEARCH AND DEVELOPMENT ADMINISTRATION

Report For
February 1975

Project Title: Preparation of a Coal Conversion Systems Technical
Data Book

ERDA Contract No. 14-32-0001-1730

I. Project Objective

The objective of this work is to provide a single, comprehensive source of data on coal conversion systems. This compilation shall be entitled The Coal Conversion Systems Technical Data Book and shall provide up-to-date data and information for the research, development, design, engineering, and construction of coal conversion processes and/or plants. Other concurrent objectives are to identify those areas where data are required and to suggest research programs that will provide the required data.

II. Summary

Liquefaction

We continued to review the literature on liquefaction to determine the current availability of data on various aspects of coal liquefaction processes.

Meetings are planned with the ERDA monitor on liquefaction (Ralph M. Parsons Co.) and other ERDA contractors involved in coal liquefaction work.

Gasification

A set of curves describing steam-oxygen gasification at 70-atm pressure is presented. The range of operating variables covers four temperatures (1750°, 1800°, 1850°, and 1900°F) and four steam/carbon molar ratios.

Carbon conversion is given as a function of solids residence time, and the product gas composition is given as a function of carbon conversion.

The computations are based on a fluid-bed model assuming that the solids and the gas are in "backmixed" flow. The associated gasification kinetics are also described.

Fluidization

The evaluation of various correlations for estimating the minimum fluidization velocity for coal and related materials is given.

Coal, Char, and Oil Shale Properties

In discussions with Penn State personnel, arrangements were made to obtain analytical data from their PSOC series for compilation in the data book. A preliminary list of large deposits (~10⁹ tons) has been prepared, for which analytical data will be obtained.

Some of the correlations used for calculating the heat of combustion of chars were evaluated by comparing the data obtained from chars from the different stages of the HYGAS operation. These chars were produced from a single lignite source.

Miscellaneous

Letters were sent out to various people involved in gasification studies for their data that can be included in the data book.

Notice to Readers of Open File

Any comments about the material presented in this report or suggestions about the format and the content of the data book as well as the priorities of the needed data are most welcome. Please direct any communications to Mr. Bipin Almaula of ERDA (202/634-6643) or to Dr. Al Talwalkar of the Institute of Gas Technology (312/225-9600, ext. 869).

III. Work Accomplished

A. LIQUEFACTION

We are continuing our literature search on coal liquefaction to determine the availability of data on various aspects of conversion of coal to liquids. The data from different reports are tabulated in various categories for easy reference for evaluation studies that are to follow.

Table 1 gives a summary of the results of the search carried out so far.

Meetings are planned with Bureau of Mines' personnel in Pittsburgh, Ralph M. Parsons Co., and Fluor Engineers & Constructors, Inc., to discuss the coal liquefaction section of the data book. The meetings will cover the following specific areas:

1. Liquefaction data available at the location
2. Availability of the other relevant information — sources and the form of available data
3. Presentation of data in a useful form
4. Expected future information that might be included in the data book
5. Data book format in general.

B. GASIFICATION

General equations have been developed at IGT that describe the kinetics of coal gasification reactions.^{1, 2} These equations can be used to develop engineering correlations that define the effects of pertinent design variables on gasification rates over a wide range of conditions applicable to many gasification processes. Moreover, the equations when combined with a suitable model of the gas/solid contacting system can be used to develop working charts that are useful for design of commercial gasification systems.

The information used in developing the kinetic equations come from laboratory thermobalance, moving-bed gasification, and fluidized-bed gasification tests performed at IGT. In addition, experimental studies performed by investigators at other laboratories have proved useful in formulating the model.

Table 1, Part 1. PRELIMINARY SAMPLE OF COAL LIQ

<u>Project/Report Title</u>	<u>Solvent Properties</u>	<u>Coal Types Studied</u>	<u>Slurry Physical Properties and Heat-Transfer Data</u>	<u>Rate Data</u>	<u>Yield Structure</u>	<u>Catalyst</u>	<u>Product Liquid Properties</u>
<u>H-COAL</u> OCR R&D Report No. 26, <u>Project H-COAL Report on Process Development</u> , Hydrocarbon Research Institute, no date	5 solvent types, hydrogenated and unhydrogenated	Illinois No. 6, Utah D-Seam, North Dakota lignite	Ultimate analyses, Sp Gr	Integral; deactivation data, pressure, temperature, solvent/coal ratios, catalyst type and size	Catalyst age, pressure, temperature, space velocity, catalyst size; solvent/coal ratios, recycle	Size, composition; Mo C, + Co O on alumina; Ni-Mo on alumina	*API, % sulfur, distillation curve, gas chromatographic data, effect of hydro-treating
<u>Consol Synthetic Fuel</u> Final Report, <u>Development of CSF Coal Liquefaction Process</u> , OCR Report No. 37, Vol. 3					Solvent/coal ratio, recycle		
<u>Start-Up and Initial Operations at Cresap Pilot Plant</u> , OCR, R&D Report No. 39, Vol. 1, Book 2	Viscosity, Sp Gr						Viscosity, carbonization data
<u>Pilot-Scale Development of the CSF Process</u> , OCR Report No. 39, Vol. 2, Book 3		Ireland mine	Viscosity, heater ΔP	Temperature, solvent type (integral)	Temperature, solvent type	Hydrogenation, catalyst aging	Sp Gr, viscosity, effect of hydro-treating
<u>Project Western Coal</u> Final Report: <u>Project Western Coal Conversion of Coal into Liquids</u> , OCR, May 1970.		Colorado high-volatile bituminous		Batch	Temperature, pressure, catalyst/solvent ratio, H ₂ /coal ratio, coal size	Mo O ₃	Sp Gr, ultimate analyses, distillation curves, % sulfur, gas chromatographic data
<u>Project Seacoke</u> Project Seacoke - Phase II Final Report, <u>Catalytic Hydrotreating of Coal-Derived Liquids</u> , OCR R&D Report No. 39, December 1966.	Anthracene, phenanthracene			Pressure, temperature, H ₂ /oil ratio for coal-derived liquids hydrogenation	Pressure, temperature, catalyst type (hydrogenation of coal-derived liquids)	Cobalt carbonyl, Co-Mo	Sp Gr, distillation curves, gas chromatographic data

BLANK PAGE

OF COAL LIQUEFACTION DATA AVAILABILITY

	<u>Product Liquid Properties</u>	<u>Product Gas Properties</u>	<u>Product Solid Properties</u>	<u>Solid/ Liquid Separation</u>	<u>Status of Development</u>	<u>Process Flow Sheet</u>	<u>Material and Energy Balance</u>	<u>Cost Data</u>
Distillation, on Mo on	*API, % sulfur, distillation curve, gas chromatographic data, effect of hydro- treating	Composition	% sulfur	Particle size distribu- tion, cyclone capacities	Pilot plant	Detailed flow sheet for commercial plant design	Detailed mass and heat balances for commercial plant	Cost estimate for commercial plant
				Filtration rates, ΔP , Hydroclone ΔP data, permeability filter cakes				
	Viscosity, carbonization data		Ash distribu- tion					
	Sp Gr., viscosity, effect of hydro- treating		Size distribu- tion, density, Fischer assay			Hydroclone ΔP , efficiency		
	Sp Gr., ultimate analysis, distilla- tion curves, % sulfur, gas chromatograph data							
	Sp Gr., distillation curves, gas chromatographic data							

E75030511a

2

Table 1, Part 2. PRELIMINARY SAMPLE OF COAL LIQUID

<u>Project/Report Title</u>	<u>Solvent Properties</u>	<u>Coal Types Studied</u>	<u>Slurry Physical Properties and Heat-Transfer Data</u>	<u>Rate Data</u>	<u>Yield Structure</u>	<u>Catalyst</u>	<u>Product Liquid Properties</u>	<u>Other</u>
Laughrey, P. W., "Symposium on Coal Hydrogenation, Design of Preheaters and Heat Exchangers for Coal Hydrogenation Plants," <u>Trans. Am. Soc. Mech. Eng.</u> 72, 385-91 (1950) May AEC 2741.								
Hirst et al., <u>Estimated Plant and Operating Costs for Producing Gasoline by Coal Hydrogenation</u> , U. S. B. M., August 1949.	Methanol	<ul style="list-style-type: none"> • Wyoming bituminous • North Dakota lignite • Montana subbituminous • Illinois bituminous • Pittsburgh seam bituminous 	Ultimate analysis				Iron oxide or iron sulfate for Pittsburgh coal. Molybdenum deposited on activated fuller's earth.	
Given et al., "The Relation of Coal Characteristics to Coal Liquefaction Behavior," Report No. 1 submitted to NSF, Agreement No. 216, Pennsylvania State Univ., March 1974.	Coal liquid Product from previous runs Hydrogenated Phenanthracene Chemical analysis	<ul style="list-style-type: none"> • Kentucky No. 11 • Mining City • Mineral • Kentucky No. 9 • Indiana No. 6 • Indiana No. 7 • Illinois No. 6 • Lower Dekoven • Illinois No. 4 	Elemental analysis	Continuous, T.	Solvent to coal ratio, % Solvation % Hydrocracking	Gulf proprietary catalyst		
"The Relation of Coal Characteristics to Coal Liquefaction Behavior," Report No. 2 submitted to NSF, Agreement No. 216, Pennsylvania State Univ., August 1974.		<ul style="list-style-type: none"> • Pittsburgh Mathias • Red Stone Koske • Lyons Mt. • Imboden • Prescott • Ohio No. 8 • Meigs Creek, No. 9 • Ohio No. 11 • Ohio No. 12 • Ohio No. 12A • Ohio No. 6 		Continuous, T.	% Solvation % Hydrocracking	Gulf proprietary catalyst	SARA, wt %	
Given et al., "Dependence of Coal Liquefaction Behavior on Coal Characteristics" Report submitted to OCR, Contract No. 14-01-0001-380, Pennsylvania State Univ., June 14, 1974.	Benzene, Anthracene Oil			Batch				

OF COAL LIQUEFACTION DATA AVAILABILITY

<u>Product Liquid Properties</u>	<u>Product Gas Properties</u>	<u>Product Solid Properties</u>	<u>Solid/ Liquid Separation</u>	<u>Status of Development</u>	<u>Process Flow Sheet</u>	<u>Material and Energy Balance</u>	<u>Cost Data</u>
			Delayed coking of the hot catch- pot bottom product	Plant size of 30,000 bbl/day. 12 plants are built in West Germany	<ul style="list-style-type: none"> • Overall flow diagram ▪ Flow sheet for various plants 	Material balance (overall plant)	Capital investment and operating cost data. 30,000 bbl/day
		Elemental analysis	Filtration	Bench-scale			
SARA, wt %		Solvation % Residue % Min. matter ash, % of demer- alized residue	Filtration	Bench-scale		Material balance on bench-scale liquefaction run	
			Filtration	Bench-scale			

E75030511b

Table 1, Part 3. PRELIMINARY SAMPLE OF COAL L

<u>Project/Report Title</u>	<u>Solvent Properties</u>	<u>Coal Types Studied</u>	<u>Slurry Physical Properties and Heat-Transfer Data</u>	<u>Rate Data</u>	<u>Yield Structure</u>	<u>Catalyst</u>	<u>Product Liquid Properties</u>
Schlesinger et al. "Relative Activity of Impregnated and Mixed Molybdenum Catalysts for Coal Hydrogenation." U. S. B. M. Report Investigation 6021.	Benzene				I. P. % catalyst	Molybdenum	
Angelovich et al. Solvents Used in the Conversion of Coal. I&EC Process Des. Develop. 9 No. 1 (1970) January.	<ul style="list-style-type: none"> • Boiling point • Density • Nonpolar solubility 	Limol coal Pittsburgh seam			Yield as a function of nonpolar solubility parameter	0.5% wet ferrous iron	
"Liquefaction and Chemical Refining of Coal" (A Battelle Energy Program Report) Battelle, Columbus, July 1974.			A Summary of Coal-Liquefaction Processes:	<ol style="list-style-type: none"> 1. Aqueous Leaching Processes 2. Solvent Refining Processes 3. Catalytic Hydrogenation Processes 4. Fischer-Tropsch Processes 5. Pyrolytic or Carbonization Processes 			
Wu and Storch, "Hydrogenation of Coal and Tar." U.S. Bureau of Mines Bull. 633, 1968.			A Review of Development of Coal and Tar Hydrogenation Technology: covers (in detail)	<ol style="list-style-type: none"> 1. History 2. Primary Hydrogenation of Coal 3. Hydrogenation of Middle Oil 4. Industrial Liquid-Phase Hydrogenation 5. Industrial Vapor-Phase Hydrogenation 6. Overall Results of Two-Phase Hydrogenation 7. Equipment 			
Hassan Hariri et al. "Kinetic Study of Thermal Dissolution of High-Volatile Bituminous Coal." Submitted to OCR. Contract No. 14-0001-271. University of Utah, 1965.	Tetralin is used. Properties of various other solvents are reported. Properties are: <ul style="list-style-type: none"> • Boiling point • % extraction • % benzene sol 		Kinetic data of solvent-extraction of coal by Tetralin is reported. Enthalpy and entropy of activation is studied, for various percentages extracted.				
Project Western Coal - 1967 Interim Reports							
Anderson et al. "Flash Heating and Plasma Pyrolysis of Coal"				A report on high-energy flash heating and hydrogen arc plasma pyrolysis of Western United States coal.			
Cheng Chen Chung, V. et al. "A Kinetic Study of Coal Extraction by Tetralin With Ultrasonic Irradiation."				Kinetics of coal extraction by 1, 2, 3, 4 tetrahydronaphthalene (tetralin) under the influence of ultrasonic waves was studied, at five different temperatures.			

TABLE OF COAL LIQUEFACTION DATA AVAILABILITY

<u>Product Liquid Properties</u>	<u>Product Gas Properties</u>	<u>Product Solid Properties</u>	<u>Solid/ Liquid Separation</u>	<u>Status of Development</u>	<u>Process Flow Sheet</u> Block diagram	<u>Material and Energy Balance</u>	<u>Cost Data</u>
--	---------------------------------------	---	---	----------------------------------	--	--	------------------

Distillation

• Mass balance of
Pittsburgh seam
coal in autoclave

E75030511c

Table 1, Part 4. PRELIMINARY SAMPLE OF COAL LIQUEF.

<u>Project/Report Title</u>	<u>Solvent Properties</u>	<u>Coal Types Studied</u>	<u>Slurry Physical Properties and Heat-Transfer Data</u>	<u>Rate Data</u>	<u>Yield Structure</u>	<u>Catalyst</u>	<u>Product Liquid Properties</u>
Wiser, W. H., A Kinetic Comparison of Coal Pyrolysis and Coal Dissolution		Utah high- volatile bituminous coal	<ul style="list-style-type: none"> • A comparison is presented of coal pyrolysis at temperatures ranging from 409° to 407°C and thermal dissolution of coal in tetralin at temperatures ranging from 350° to 450°C. • A model is presented that relates the two processes and explains the significance of the similarities between the two processes. 				
Qader, S. A. et al., "Kinetics of the Hydro- Removal of Sulfur, Oxygen, and Nitrogen From a Low-Temperature Coal-Tar." OCR Contract 14-01-0001-271, University of Utah.			Kinetics of hydro-removal of S, O, N are determined.				
Project Western Coal. Research and Development Report No. 18, "Conversion of Coal Into Liquids, Final Report." OCR Contract No. 14-01-0001-271, University of Utah.			Fundamental kinetic data for pyrolysis, solvent extraction, and hydrogenation. ZnCl ₂ used for hydrogenation catalyst.				
"Solvent Refining of Coal: Background Information on Solvent Extraction of Coal for EPRL." Contract No. RP-123-1-6, August 1974.	Anthracene oil • API • Elemental analysis • Distillation curves • Analysis of cuts • Heating value	• West Kentucky-14 • Illinois No. 6	Coal solution, wt %		Continuous, P. T. coal feed rate	Noncatalytic	• API gravity • C. H. S. N ₂ phenol wt % • Viscosity • Softening pt. • Nitrogen content • Heating value
Liquefaction of Kaiparowits Coal by Solvent Refined Coal Process and H-COAL Processing for EPRI (Electric Power Research Institute) Contract No. RP-123-2, October 1974.	Anthracene oil • API gravity • Elemental analysis • Distillation • Analysis of cuts Laboratory-scale experiments were carried out using: 1. Solvent-refined coal process 2. High- and low-severity H-COAL Process	Kaiparowits coal (Utah area)			Low severity High severity	Noncatalytic for solvent-refined coal process Commercial catalyst for H-COAL	
Johnson, C. A. et al., Production of Gasoline From Australian Brown Coal by the H-COAL Process. Proceedings of Eight World Petroleum Congress (1972).		Australian brown coal				Commercial hydrogenation catalyst	

—* COAL LIQUEFACTION DATA AVAILABILITY

<u>Product Liquid Properties</u>	<u>Product Gas Properties</u>	<u>Product Solid Properties</u>	<u>Solid/ Liquid Separation</u>	<u>Status of Development</u>	<u>Process Flow Sheet</u>	<u>Material and Energy Balance</u>	<u>Cost Data</u>
497°C J°C. of the							

- API gravity
- C, H, S, N₂
- phenol wt %
- Viscosity
- Softening pt.
- Nitrogen content
- heating value

Flow. mass
spectroscopic
analysis (vapor-
phase chroma-
tography)

E75030511d

2

Table 1, Part 5. PRELIMINARY SAMPLE OF COAL LI

<u>Project/Report Title</u>	<u>Solvent Properties</u>	<u>Coal Types Studied</u>	<u>Slurry Physical Properties and Heat-Transfer Data</u>	<u>Rate Data</u>	<u>Yield Structure</u>	<u>Costs</u>	<u>Product Liquid Properties</u>	<u>Pro C Prod</u>
"Evaluation of Project H-COAL by American Oil Co." prepared for OCR Contract No. 14-01-0001-1188, American Oil Project No. 6120 April-August 1967.			This report compares the economic estimates made by Hydrocarbon Research Inc. and by American Oil Co. The economic evaluation is discussed in detail.					
"Markovitz, J. A. et al. Special Equipment in the Coal-Hydrogenation Demonstration Plant" U. S. Bureau of Mines (1950) January AEC 2726.					For 95% conversion residence time is approx 1 hr		1-2% iron oxide or 0.05% tin oxalate	

AMPLE OF COAL LIQUEFACTION DATA AVAILABILITY

<u>Product Liquid Properties</u>	<u>Product Gas Properties</u>	<u>Product Solid Properties</u>	<u>Solid/ Liquid Separation</u>	<u>Status of Development</u>	<u>Process Flow Sheet</u>	<u>Material and Energy Balance</u>	<u>Cost Data</u>
				2 bench-scale units 1 pilot plant	Block diagram for various sections of the process		Economic estimates (based on 30,000 bbl/day) 1967 cost, also on 100,000 bbl/day
				A demonstration plant at Louisiana, Mo.	<ul style="list-style-type: none"> • Detailed diagram of various equip- ment used in the plant • Overall flow diagram of the process 		

E75030511e

2

1. Discussion of General Coal Gasification Reactions

a. Devolatilization

When a coal or coal char containing volatile matter is initially subjected to an elevated temperature, a series of complex physical and chemical changes occur in the coal's structure, accompanied by thermal pyrolysis reactions that results in devolatilization of certain coal components. The distribution of the evolved products of the reactions, which initiate at less than 700°F and can be considered to occur almost instantaneously at temperatures greater than 1300°F, is generally a function of the temperature, pressure, and gas composition existing during devolatilization and of the subsequent thermal and environmental history of the gaseous phase (including entrained liquids) prior to quenching.

b. Rapid Rate Methane Formation

When devolatilization occurs in the presence of a gas containing hydrogen at an elevated pressure, in addition to thermal pyrolysis reactions, coals or coal chars containing volatile matter also exhibit a high although transient reactivity for methane formation. Although some investigators have suggested that this process occurs simultaneously with thermal pyrolysis reactions, studies done with a greater time resolution indicated that this rapid-rate methane formation occurs at a rate which is at least an order of magnitude slower than devolatilization. In this sense it occurs after devolatilization.

The amount of carbon gasified to methane during the transient high reactivity increases significantly with increases in hydrogen partial pressure. At temperatures greater than 1700°F, the transient reactivity for rapid-rate methane formation exists only briefly.

c. Char Gasification

After the devolatilization and rapid-rate methane formation stages are completed, char gasification occurs at a relatively slow rate. The differential rates of reaction of devolatilized coal chars are a function of temperature, pressure, gas composition, carbon conversion, and prior history.

The coal gasification kinetic model, therefore, assumes that the overall gasification occurs in three consecutive stages: 1) devolatilization, 2) rapid-rate methane formation, and 3) low-rate gasification. The reactions in the three stages are independent. Further, a feed coal contains two types of carbon - volatile carbon and base carbon. Volatile carbon can be evolved solely by thermal pyrolysis, independent of the gaseous medium. Base carbon

remains in the coal char after devolatilization is complete. This carbon can be subsequently gasified in either the rapid-rate methane formation stage or the low-rate gasification stage.

Initial amounts of volatile and base carbon are estimated from standard analyses of the feed coal char:

$$\begin{aligned} C_v \text{ (volatile carbon), grams/gram feed coal} \\ &= C_t^\circ \text{ (total carbon), grams/gram feed coal} \\ &- C_b^\circ \text{ (base carbon), grams/gram feed coal} \end{aligned} \quad (1)$$

where C_t° represents the total carbon in the feed coal obtained from an ultimate analysis, and C_b° represents the carbon in the fixed carbon fraction of the feed coal as determined in a proximate analysis. Note that C_b° does not equal the fixed carbon fraction because the fixed carbon fraction includes, in addition to carbon, other organic coal components not evolved during standard devolatilization.

When an analysis of the fixed carbon fraction is not available or an estimate of organic coal components present in the fixed carbon fraction cannot be made, then C_b° can be approximated with the expression:

$$C_b^\circ = 0.96 \text{ (fixed carbon fraction), grams/gram feed coal.}$$

The base carbon conversion fraction, X , is defined as -

$$X = \frac{\text{base carbon gasified}}{\text{base carbon in feed coal char}} = \frac{C_b^\circ - C_b}{C_b^\circ} \quad (2)$$

where C_b = base carbon in coal char at an intermediate level of gasification, grams/gram feed coal char.

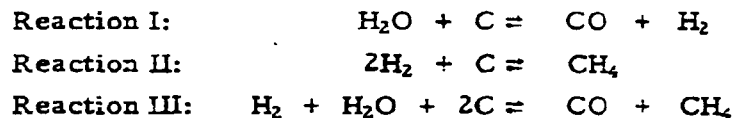
This definition is used in correlations in the following section to describe carbon gasification kinetics in the low-rate regime.

2. Low-Rate Gasification Kinetics

As discussed above, for practical purposes coal chars undergo low-rate gasification only after the devolatilization and rapid-rate methane formation reactions are completed. Results obtained with the thermobalance indicate that at greater than 1500°F char reactivity over a major range of carbon conversion in the low-rate stage is substantially the same whether

devolatilization occurs in nitrogen or in a gasifying atmosphere under the same conditions. Therefore, in this model, low-rate char gasification is considered as a process essentially independent of devolatilization conditions with one important exception: the temperature of devolatilization. It was found that the reactivity of a char at a given temperature, T , decreases with increasing previous treatment temperature, T_0 , when $T_0 > T$. This effect is quantitatively represented in the correlations below.

Three basic reactions are assumed to occur with char in gases containing steam and hydrogen:



Reaction I is the conventional steam-carbon reaction which is the only one that occurs in pure steam at elevated pressures or with gases containing steam at low pressure. Although at elevated temperatures this reaction is affected by thermodynamic reversibility only for relatively high steam conversions, the reaction is severely inhibited by the poisoning effects of hydrogen and carbon monoxide at steam conversions far removed from equilibrium for this reaction.

Reaction II, the only reaction that could occur in pure hydrogen or in hydrogen-methane mixtures, depends greatly on the hydrogen partial pressure. At elevated pressures its rate is directly proportional to the hydrogen partial pressure.

The stoichiometry of Reaction III limits its occurrence to systems in which both steam and hydrogen are present. Although this reaction is the stoichiometric sum of Reactions I and II, this model considers it to be a third, independent gasification reaction. Reaction III, arbitrarily assumed to occur in the development of this model to facilitate correlations of experimental data, has also been suggested by other investigators.

The correlations developed to describe kinetics in the low-rate gasification stage are summarized as follows:

$$dX/dt = f_L k_T (1 - X)^{2/3} \exp(-\alpha X^2) \quad (3)$$

where -

$$k_T = k_I + k_{II} + k_{III} \quad (4)$$

Here, k_I , k_{II} , and k_{III} are rate constants for the individual reactions considered. It is assumed that each of the three reactions occurs independently but that the rate of each is proportional to the same surface area term, $(1 - X)^{2/3}$ and surface reactivity term, $\exp(-\alpha X^2)$.

Individual parameters in Equations 3 and 4 are defined as functions of temperature and pressure according to -

$$f_L = f_0 \exp(8467/T_0) \quad (5)$$

$$k_I = \frac{\exp(9.0201 - 31,705/T) \left(1 - \frac{P_{CO} P_{H_2}}{P_{H_2O} K_I^E} \right)}{\left[1 + \exp(-22,2160 + 44,787/T) \left(\frac{1}{P_{H_2O}} + 16.35 \frac{P_{H_2}}{P_{H_2O}} + 43.5 \frac{P_{CO}}{P_{H_2O}} \right) \right]^2} \quad (6)$$

$$k_{II} = \frac{P_{H_2}^2 \exp(2.6741 - 33,076/T) \left(1 - \frac{P_{CH_4}}{P_{H_2}^2 K_{II}^E} \right)}{\left[1 + P_{H_2} \exp(-10.4520 + 19,976/T) \right]} \quad (7)$$

$$k_{III} = \frac{P_{H_2}^{1/2} P_{H_2O} \exp(12.4463 - 44,544/T) \left(1 - \frac{P_{CH_4} P_{CO}}{P_{H_2} P_{H_2O} K_{III}^E} \right)}{\left[1 + \exp(-6.6696 + 15,198/T) \left(P_{H_2}^{1/2} + 0.85 P_{CO} + 18.62 \frac{P_{CH_4}}{P_{H_2}} \right) \right]^2} \quad (8)$$

$$a = \frac{52.7 P_{H_2}}{1 + 54.3 P_{H_2}} + \frac{0.521 P_{H_2}^{1/2} P_{H_2O}}{1 + 0.707 P_{H_2O} + 0.50 P_{H_2}^{1/2} P_{H_2O}} \quad (9)$$

where -

$K_I^E, K_{II}^E, K_{III}^E$ = equilibrium constants for Reactions I, II, and III, considering carbon as graphite

T = reaction temperature, °R

T_0 = maximum temperature to which char has been exposed prior to gasification, °R (if $T_0 < T$, then a value of $T_0 = T$ is used in Equation 5)

$P_{H_2}, P_{H_2O}, P_{CO}$ = partial pressures of H_2, H_2O, CO , and CH_4 , atm

P_{CH_4}

f_0 = relative reactivity factor for low-rate gasification which depends on the particular carbonaceous solid

Values of f_0 are based on the definition $f_0 = 1.0$ for a specific batch of air-pretreated Ireland mine coal char. Samples of this coal char obtained from different air-pretreatment tests exhibited some variations in reactivity as determined by thermobalance tests conducted at standard conditions. The values of f_0 so determined ranged from approximately 0.88 to 1.05. Results of tests made with the thermobalance, using a variety of coals and coal chars, have indicated that the relative reactivity factor, f_0 , generally tends to increase with decreasing rank although individual exceptions to this trend exist. Values have been obtained which range from 0.3 for a low-volatile bituminous coal char to about 10 for a North Dakota lignite.

The range of the relative reactivity factor, f_0 , for different types of coals will be presented in future reports of this study.

3. Steam-Oxygen-Char Gasification in Fluidized Bed

In many coal gasification processes, coal char is gasified with steam and oxygen to produce a synthesis gas. Because of its wide applications, we initially applied IGT's gasification model to develop information useful in the designing of fluidized-bed reactors to gasify char with steam-oxygen mixtures.

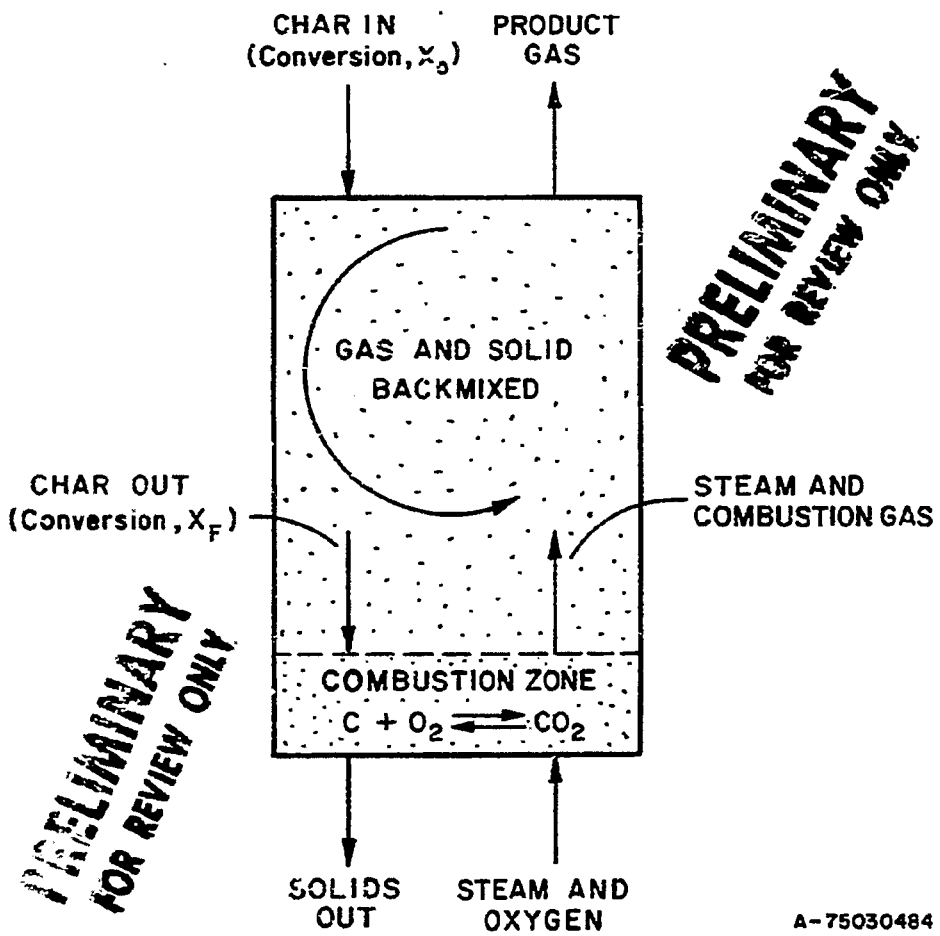
a. Fluidized-Bed Model

Before using the kinetics correlations, it is necessary to describe the physical nature of the gas-solid contacting in the fluidized bed. Figure 1

shows the fluidized-bed model used in developing the information presented here.



EDRA	_____
PAGE	_____
REVISION No.	_____
DATE	_____



A-75030484

Figure 1. FLUIDIZED-BED MODEL

The model assumes that -

1. The fluidized bed consists of two distinct zones: a combustion zone and a gas-solid backmixed zone.
2. The combustion zone is assumed to have negligible volume; the only reaction in this zone is that of carbon combustion to produce carbon dioxide. Char that undergoes combustion in this zone passes out of the system, but not back to the backmixed zone. Both combustion gases and steam go up from this zone into the backmixed zone. However, there is enough unburned char circulation from this zone to the backmixed zone so as to carry heat evolved from combustion into the bulk of the bed.
3. In the remainder of the fluidized bed, the gas and the solids are perfectly backmixed, and essentially all rate-controlling steam-carbon and hydrogen-carbon reactions occur in this zone.
4. The composition of the gases and the solids throughout the backmixed zone are the same as those of the char entering the combustion zone and the product gas exiting the gasifier.

Operating experience with the pilot-plant-scale fluidized bed at IGT indicates that in a well fluidized bed, with an L/D ratio of under 4, the assumption of both gas and solid being completely backmixed is in good agreement with experimental evidence. For cases where the gas is backmixed but the solids are in plug flow, a conversion factor will be presented next month to adjust the information below, which is for the model in which both the gas and the solid are perfectly backmixed.

Besides defining the above two models - kinetic and gas-solid contacting - a few more conditions have to be fixed before a steam-oxygen-char gasification system can be characterized. The following conditions have been arbitrarily fixed for ease in calculating and presenting the design information given later in this section:

1. The feed to the gasification system is a coal char that does not contain any volatile carbon; therefore, no devolatilization reactions occur in the system. Further, none of the base carbon has been converted in the feed char; that is, X_0 , the base carbon conversion fraction, equals 0. Later on in this study, a method will be presented that will allow the consideration of cases wherein the feed char $X_0 > 0$ in the feed char.
2. The feed coal char has been assigned a relative reactivity factor for low-rate gasification, f_0 , of unity. This corresponds to the reactivity for air-pretreated Ireland mine coal char. A procedure to handle feeds having a relative reactivity factor less than or more than unity will be described later in this study. (The relative reactivity factors for different ranks of coals will also be presented later in this study.)

3. The gasification system operates adiabatically at the specified temperature. The heat requirement for the system to maintain the temperature is provided by combustion of the feed oxygen with a part of coal char. Heat losses from the system are assumed to be negligible.
4. The product gas is assumed to satisfy the water-gas shift reaction equilibrium at the system operating temperature and pressure.

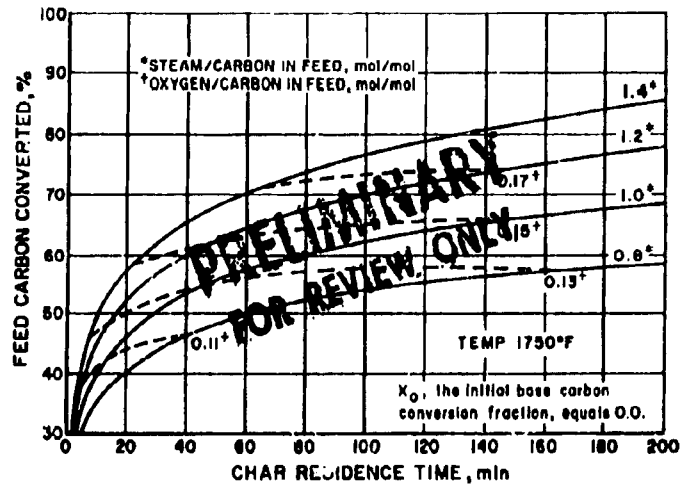
b. Carbon Conversion Versus Solids Residence Time Curves

With the two models and the above assumptions, the steam-oxygen-char gasification system can now be characterized. The design information presented here is in a form that can be readily used by a design engineer to size a gasifier and specify steam and oxygen feeds.

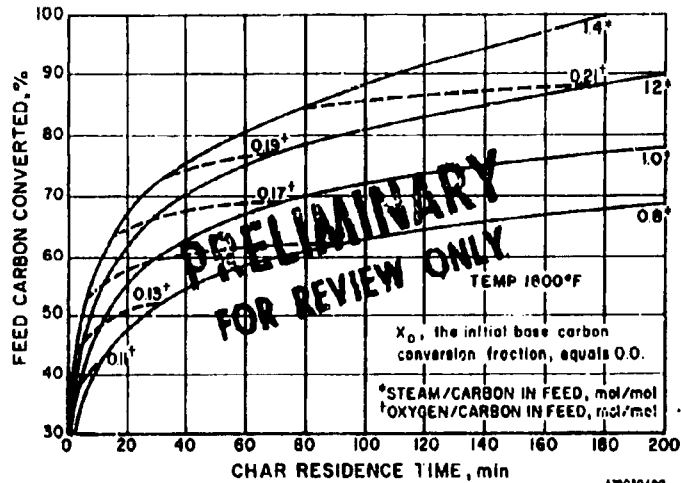
For a given gasification temperature and 70-atm pressure, Figure 2 presents curves that give the char residence time required to achieve a specified feed carbon conversion at different steam feeds to the gasifier. The charts also show the amount of oxygen that is required in the feed to maintain adiabatic operation at any operating condition. The steam and the oxygen feeds have been normalized with respect to carbon in the char feed to make the charts more generally applicable. Normally, to achieve 100 % feed carbon conversion, the solids residence time required would be infinite. However, because part of the char feed is combusted with oxygen to supply heat to the system, it is possible to achieve 100 % conversion and yet have a finite solids residence time.

c. Gas Composition Versus Carbon Conversion Curves

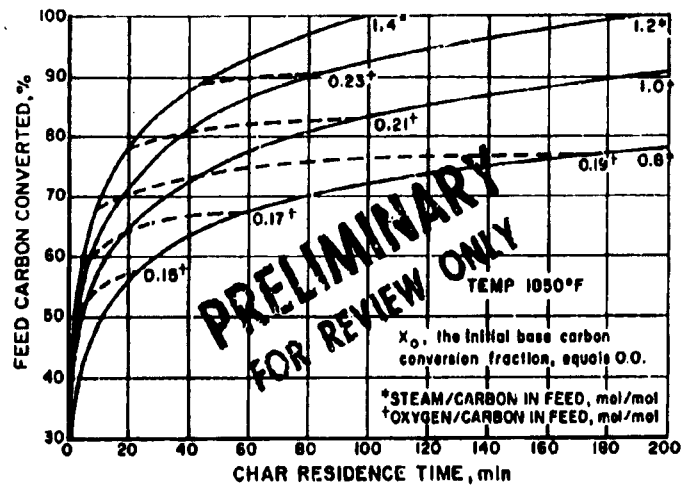
Once the gasifier has been sized for a given carbon conversion, feed steam, and operating temperature, it is necessary to know the quantity and the composition of the product gas. The curves in Figures 3, 4, 5, and 6 show the total number of moles of product gas as well as the composition of the product gas as a function of feed carbon conversion for a given steam feed and operating temperature. Once again, for a generalized application, the curves have been normalized with respect to the carbon in the char feed to the gasifier. Additionally, the gas composition curves are shown on a cumulative percentage basis.



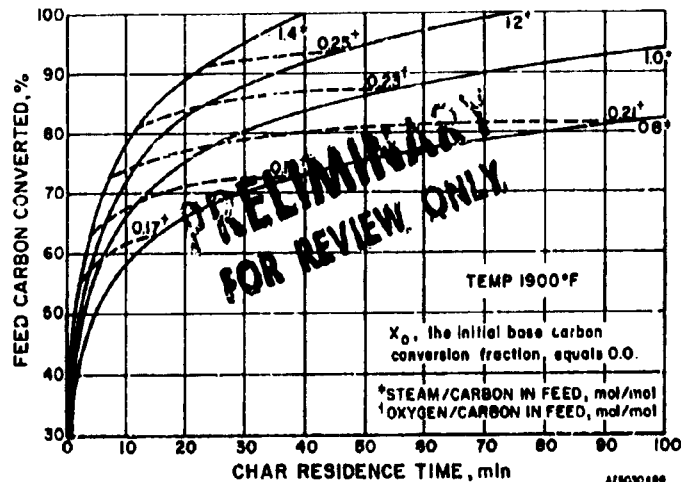
A75030487



A75030490



A-75030489



A75030488

Figure 2. STEAM-OXYGEN GASIFICATION OF DEVOLATILIZED IRELAND MINE BITUMINOUS CHAR AT VARIOUS TEMPERATURES AND AT 70-atm PRESSURE

2/75



EDRA
PAGE
REVISION No.
DATE

8964



EDRA	_____
PAGE	_____
REVISION No.	_____
DATE	_____

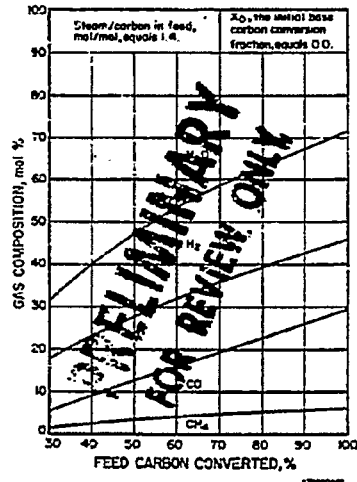
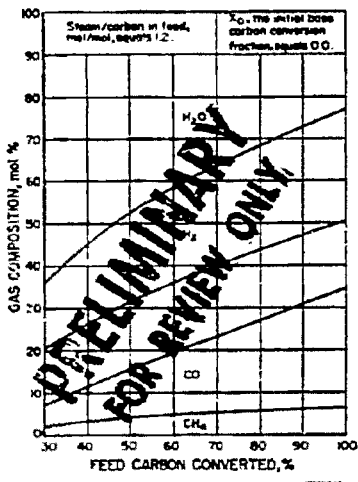
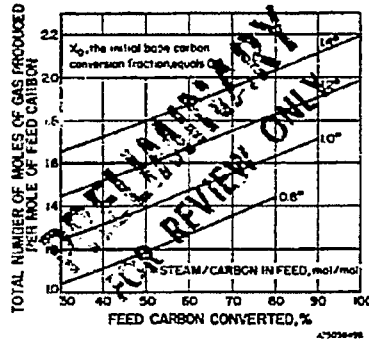
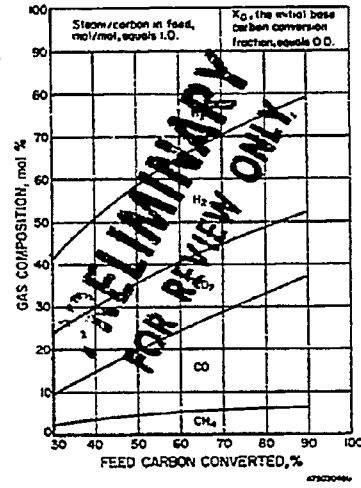
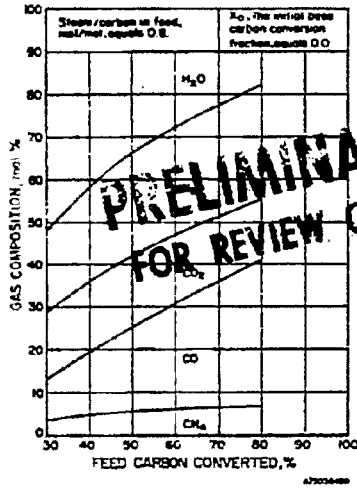


Figure 3. STEAM-OXYGEN GASIFICATION – PRODUCT GAS COMPOSITIONS (Temperature = 1750°F; Pressure = 70 atm)



EDRA	_____
PAGE	_____
REVISION No.	_____
DATE	_____

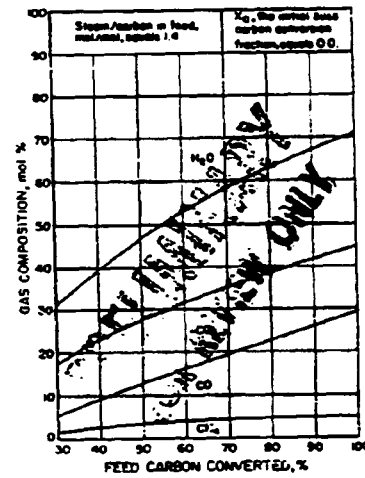
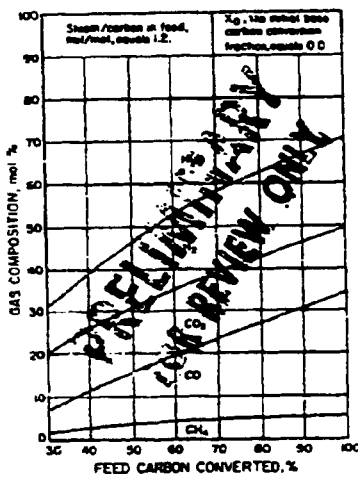
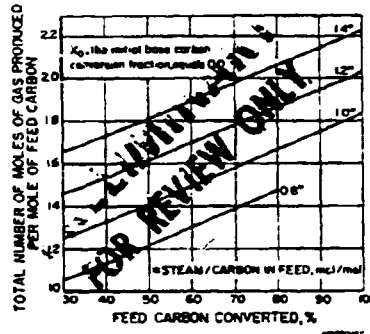
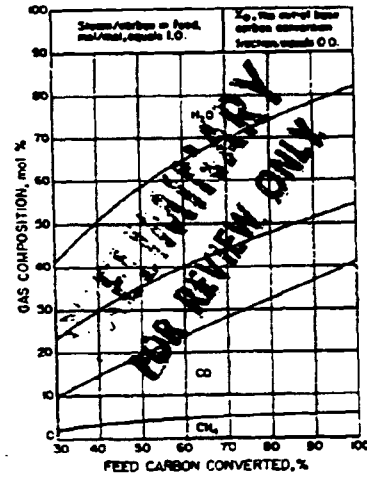
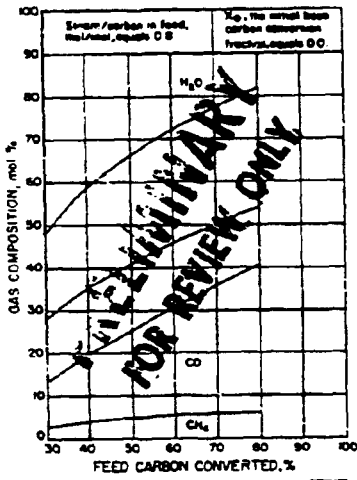


Figure 4. STEAM-OXYGEN GASIFICATION – PRODUCT GAS COMPOSITIONS
(Temperature = 1800°F; Pressure = 70 atm)



EDRA	_____
PAGE	_____
REVISION No.	_____
DATE	_____

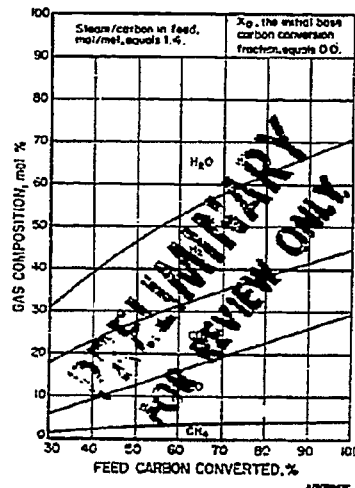
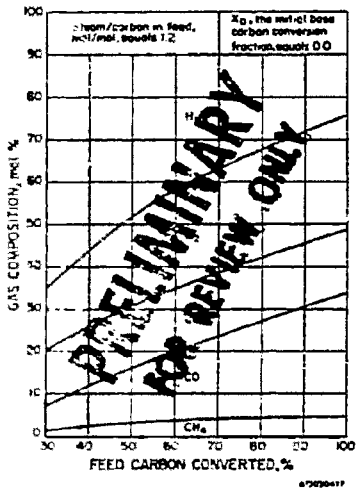
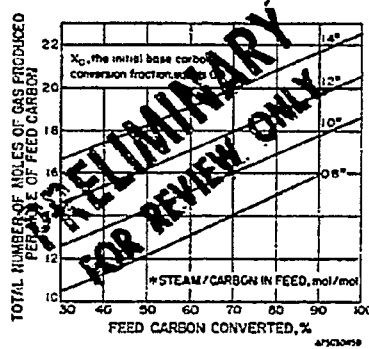
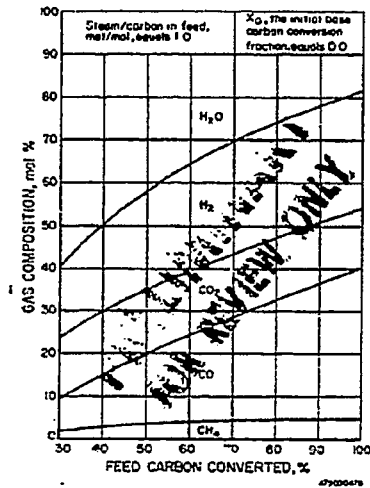
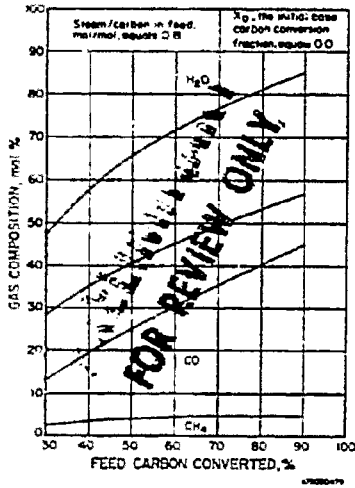


Figure 5. STEAM-OXYGEN GASIFICATION – PRODUCT GAS COMPOSITIONS
 (Temperature = 1850 °F; Pressure = 70 atn)



EDRA	_____
PAGE	_____
REVISION No.	_____
DATE	_____

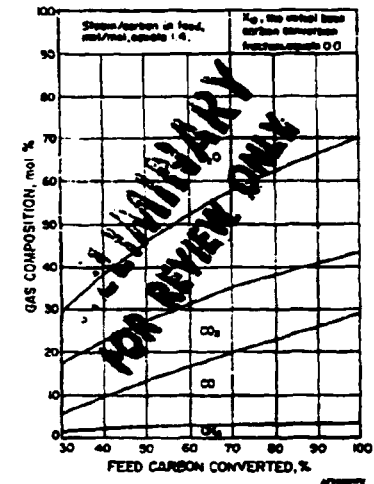
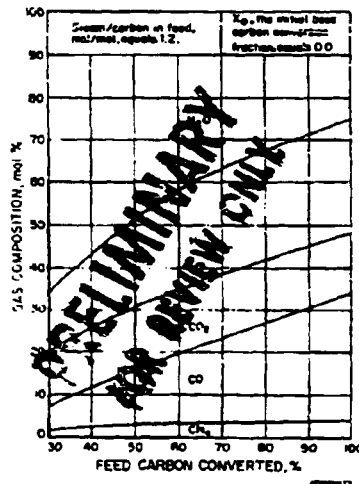
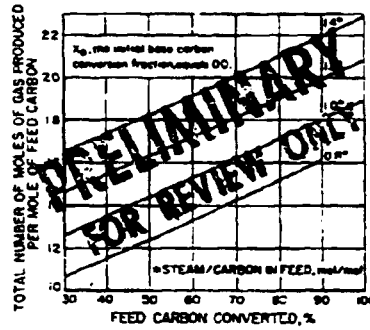
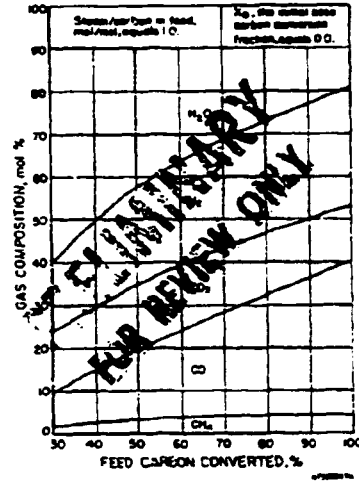
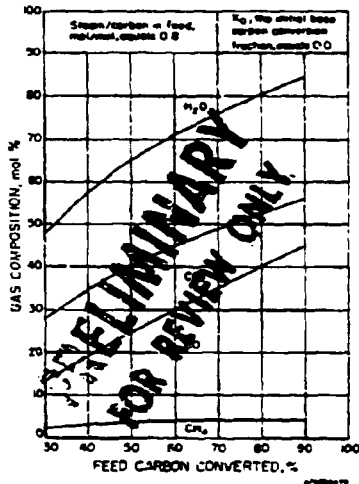


Figure 6. STEAM-OXYGEN GASIFICATION - PRODUCT GAS COMPOSITIONS (Temperature = 1900°F; Pressure = 70 atm)

We should note that the product gas does not contain any hydrogen sulfide or nitrogen. Any nitrogen or other inerts in the feed oxygen can be directly added to the product gas as they would normally pass through the gasifier without any changes. The amount of sulfur evolved from the feed char, however, depends on various other parameters; in this section, we have assumed that the sulfur in the feed char does not react in the system. Later in this study, a procedure for the accounting of the evolution of sulfur from feed char will be included.

In the next monthly report, we will include conversion factor charts to account for —

1. A feed char in which $X_0 \neq 0$
2. A gas-solid contacting model in which solids are in plug flow
3. Evolution of sulfur from feed char.

We will also give an example of a worked-out design that will show the use of the design information presented up to now.

References Cited

1. Johnson, J. L., "Kinetics of Bituminous Coal Char Gasification With Gases Containing Steam and Hydrogen," in Coal Gasification, ACS Advances in Chemistry Series No. 131, 145-78 (1974).
2. Pyrcioch, E. J., Feldkirchner, H. L., Tsaros, C. L., Johnson, J. L., Bair, W. G., Lee, B. S., Schora, F. C., Huebler, J., and Linden, H. R., "Production of Pipeline Gas by Hydrogasification of Coal, Vol. I, 1954-1964," IGT Res. Bull. No. 39. Chicago, November 1972.

C. FLUIDIZATION

1. Evaluation of Minimum Fluidization Correlations

A comprehensive list of published correlations to estimate the minimum fluidization velocity, using the physical properties of the fluidizing medium and solids, is shown in Table 2. Except for the correlations by Baerg³ and Narasimhan,¹⁹ the remaining correlations can be shown to be similar in form under certain conditions. The correlations containing similar-form fluidization parameters differ by the value of their coefficients and exponents, which were usually determined to be adequately descriptive of the fluidization system under study.

Table 2, Part 1 SOME PUBLISHED CORRELATIONS TO PREDICT MINIMUM FLUIDIZATIO

Investigators	Bed Diameter inches	Fluidized Solids	Particle Diameter inches	Fluidizing Medium	Proposed Correlation
Wilhelm and Kwauk ²⁵	2.97 and 5.75	Sea sand, socony beads, glass beads, lead shots, etc.	0.0116-0.0197	Air, water	Graphical correlation
Johnson E ¹⁰	--	--	--	--	$U_{mf} = \frac{D_p^2 g (\rho_s - \rho_g)}{18\mu} \left[\frac{\epsilon_{mf}}{1 + 0.5} \right]$ for Re
					$U_{mf} = 0.171 D_p \omega \left(\frac{\epsilon_{mf}}{1 - \epsilon_{mf}} \right)^3 \left[\frac{\epsilon_{mf}}{\mu (1 - \epsilon_{mf})} \right]$ for Re
Baerg et al. ³	5.5	Iron powder, sand, Scochlike beads, alumina cracking catalyst	0.00237-0.0345	Air	$U_{mf} = \frac{0.36}{\rho_g} (D_p \rho_B)^{1.23}$ for Re
Miller and Logwnuk ¹⁸	2.0	SiC ₂ , SiO ₂ , silica gel, Al ₂ O ₃	0.0038-0.0098	CO ₂ , air, ethane, He	$U_{mf} = 0.00125 \frac{D_p^2 (\rho_s - \rho_g)^{0.9} \rho_g}{\mu}$ for Re
van Heerden et al. ²³	3.35	Coke, iron oxide, carborundum	0.0038-0.0259	CO ₂ , air, Ar, CH ₄ , town gas	$U_{mf} = 0.00123 \frac{D_p^2 \rho_B g}{E\mu}$ for Re
Zenz ²⁶	--	--	--	--	Graphical correlation
Goroshko et al. ⁹	--	--	--	--	$U_{mf} = \frac{\mu}{\rho_g D_p} \frac{Ar}{150 \frac{(1 - \epsilon_{mf})}{\epsilon_{mf}^3} + 1}$ where $Ar = g D_p^3 \rho_g (\rho_s - \rho_g) \mu^{-2}$
Leva ¹⁵	2.5 and 4	Sand, catalyst, anthracite	0.00202-0.03819	Air, He, CO ₂	$U_{mf} = \frac{0.00088 D_p^{1.82} (\rho_s - \rho_g)^{0.94} g}{\rho_g^{0.06} \mu^{0.88}}$ for Re

FORMULAS TO PREDICT MINIMUM FLUIDIZATION VELOCITY

Fluidizing
Medium

Proposed Correlation

water

Graphical correlation

$$U_{mf} = \frac{D_p^2 \omega^2 g (\rho_s - \rho_g)}{18\mu} \left[\frac{\epsilon_{mf}^5}{1 + 0.5(1 - \epsilon_{mf})} \right]$$

for $Re_p < 2$

$$U_{mf} = 0.171 D_p \omega \left(\frac{\epsilon_{mf}}{1 - \epsilon_{mf}} \right)^3 \left[\frac{g^2 \rho_g \epsilon_{mf}^6}{\mu (1 - \epsilon_{mf}) \{ 1 + 0.5(1 - \epsilon_{mf}) \}} \right]^{1/3}$$

for $Re_p > 2$

$$U_{mf} = \frac{0.361}{\rho_g} (D_p \rho_B)^{1.23}$$

for $Re_p < 20$

O₂, air,
He

$$U_{mf} = 0.00125 \frac{D_p^2 (\rho_s - \rho_g)^{0.9} \rho_g^{0.1} g}{\mu}$$

for $Re_p < 5$

O₂, air,
CH₄,
inert gas

$$U_{mf} = 0.00123 \frac{D_p^2 \rho_{Bm} g}{B\mu}$$

for $Re_p < 13$

Graphical correlation

$$U_{mf} = \frac{\mu}{\rho_g D_p} \frac{Ar}{150 \frac{(1 - \epsilon_{mf})}{\epsilon_{mf}^3} + \left(\frac{1.75}{\epsilon_{mf}^3} Ar \right)^{1/2}}$$

where

$$Ar = g D_p^3 \rho_g (\rho_s - \rho_g) / \mu^2$$

r. He,
O₂

$$U_{mf} = \frac{0.00088 D_p^{1.82} (\rho_s - \rho_g)^{0.94} g}{\rho_g^{0.06} \mu^{0.88}}$$

for $Re_p < 10$

Table 2, Part 2. SOME PUBLISHED CORRELATIONS TO PREDICT MINIMUM FLUIDIZATION

Investigators	Bed Diameter, inches	Fluidized Solids	Particle Diameter, inches	Fluidizing Medium	Proposed Correlation
Narasimhan ¹⁹	--	--	--	--	$U_{mf} = \frac{42.9\mu}{D_p \rho_g} (0.231 \log D_p)$ $\left[(1 + 2.12 \times 10^{-5} D_p) \right]$ <p>where</p> $N_{Re_t} = D_p U_t \rho_g / \mu$
Frantz ⁸	1-12	Catalyst, sand	0.0018-0.012	N ₂ , Ar, H ₂ , ethane, and mixture of gases	$U_{mf} = 0.001065 \frac{D_p^2 (\rho_s - \rho_g)}{\mu}$
Wen and Yu ²⁴	4	Glass balls and steel balls	0.08-0.25	Water	$U_{mf} = \left[\frac{\mu}{\rho_g D_p} \right] \left[\sqrt{\{ (3) \dots \}} \right]$ <p>where</p> $N_{Ga} = \frac{D_p^3 \rho_g (\rho_s - \rho_g) g}{\mu^2}$
Davies and Richardson ⁶	--	Catalysts	--	Air	$U_{mf} = 0.00078 D_p^2 (\rho_s - \rho_g)$
Kunii and Levenspiel ¹⁴	--	--	--	--	$U_{mf} = \frac{(\phi D_p)^2 (\rho_s - \rho_g) g}{150 \mu}$ $U_{mf} = \left(\frac{\phi D_p}{1.75} \frac{(\rho_s - \rho_g)}{\rho_g} \right) g$ $\frac{1.75 D_p \rho_g}{\mu \phi \epsilon_{mf}^3} U_{mf}^2 + \frac{150 (1 - \epsilon_{mf})}{\phi^2 \epsilon_{mf}^3} = \frac{D_p^2 (\rho_s - \rho_g)}{\mu}$

EQUATIONS TO PREDICT MINIMUM FLUIDIZATION VELOCITY

Fluidizing Medium	Proposed Correlation
--	$U_{mf} = \frac{42.9\mu}{D_p \rho_g} (0.231 \log D_p + 1.417) \times$ $[(1 + 2.12 \times 10^{-5} D_p^{-0.55} N_{Re_t})^{1/2} - 1]$ <p>where</p> $N_{Re_t} = D_p U_t \rho_g / \mu$
N ₂ , Ar, H ₂ , ethane, and mixture of gases	$U_{mf} = 0.001065 \frac{D_p^2 (\rho_s - \rho_g) g}{\mu}$ <p>for Re_p < 32</p>
Water	$U_{mf} = \left[\frac{\mu}{\rho_g D_p} \right] \left[\sqrt{\{(33.7)^2 + 0.0408 N_{Ga}\}} - 33.7 \right]$ <p>where</p> $N_{Ga} = \frac{D_p^3 \rho_g (\rho_s - \rho_g) g}{\mu^2} \equiv Ar$
Air	$U_{mf} = 0.00078 D_p^2 (\rho_s - \rho_g) g / \mu$
--	$U_{mf} = \frac{(\omega D_p)^2 (\rho_s - \rho_g) g}{150 \mu} \left(\frac{\epsilon_{mf}^3}{1 - \epsilon_{mf}} \right)$ <p>for Re_p < 20</p> $U_{mf} = \left(\frac{\omega D_p}{1.75} \frac{(\rho_s - \rho_g)}{\rho_g} g \epsilon_{mf}^3 \right)^{1/2}$ <p>for Re_p > 1000</p>
	$\frac{1.75 D_p \rho_g}{40 \epsilon_{mf}^3} U_{mf}^2 + \frac{150 (1 - \epsilon_{mf})}{\omega^2 \epsilon_{mf}^3} U_{mf}$ $= \frac{D_p^2 (\rho_s - \rho_g) g}{\mu}$ <p>for 20 < Re_p < 1000</p>

B75030512b

2

Table 2, Part 3. SOME PUBLISHED CORRELATIONS TO PREDICT MINIMUM FLUIDIZATION

Investigators	Bed Diameter, inches	Fluidized Solids	Particle Diameter, inches	Fluidizing Medium	Proposed Correlation
Pillai and Raja Rao ²¹	2.9	Al-powder, iron powder, sand, polystyrene	0.0023-0.0434	Air	$U_{mf} = \frac{0.000701 D_p^2}{\mu}$
Kumar and Sen Gupta ¹³	2.2	Mixtures of salt, sand, sugar, magnetite in different combinations	--	Air	$U_{mf} = \frac{0.0054\mu}{D_p \rho_g} \left(\frac{D_{av}^3 \rho_g}{\mu} \right)$

PREDICT MINIMUM FLUIDIZATION VELOCITY

Proposed Correlation

$$U_{mf} = \frac{0.000701 D_p^2 (\rho_s - \rho_g) g}{\mu}$$

for $Re_p < 20$

$$U_{mf} = \frac{0.0054\mu}{D_p \rho_g} \left(\frac{D_{av}^3 \rho_g (\rho_{s_{av}} - \rho_g) g}{\mu^2} \right)^{0.73}$$

B75030512c

2

The mathematical similarities between a few of the generally used correlations are discussed in the Appendix.

During the past month, a computer program was written to calculate minimum fluidization velocities using some of the well-known correlations and to compare them with published data on coal and related materials. The sources and the extent of available experimental data on these materials are shown in Table 3. The computer plots comparing the calculated values with the measured values are shown in Figures 7 through 11. Several interesting observations can be drawn from these figures

It can be seen that the calculated values for $Re_p < 20$ using Frantz's⁸ and Kunii-Levenspiel's¹⁴ correlations, shown in Figures 7 and 8, respectively, show good agreement with the measured minimum fluidization velocities. It is obvious from Figures 7 and 8 that there are certain sets of data, for example the measured values by Leva *et al.*,¹⁶ Feldmann *et al.*,⁷ Jones *et al.*,¹¹ etc., that are significantly different from the calculated values. The reasons for their discrepancies are discussed in subsequent paragraphs. On the other hand, both Leva's¹⁵ and Wen and Yu's²⁴ correlations, shown in Figures 10 and 9, respectively, in general, calculate a lower velocity than the measured data. This difference can be explained by comparing the coefficients of Frantz's⁸ correlation with those of Leva's¹⁵ and Wen and Yu's²⁴ correlation as shown in the Appendix. It is conceivable that the empirical coefficient in Frantz's correlation⁸ is adequately descriptive of the type of solids considered in his investigation. By comparing the coefficients of the correlations as shown in the Appendix, it is obvious that Wen and Yu's²⁴ correlation will predict about 42% lower minimum fluidization velocity compared with Frantz's⁸ calculated value for $Re_p < 20$. Similarly, Leva's correlation¹⁵ will result in values that are about 20% less than those calculated from Frantz's⁸ correlation. This implies that the coefficients in both Leva's¹⁵ and Wen and Yu's²⁴ correlations can be adjusted to calculate sufficiently higher value to improve their comparison with published data on coal and related materials.

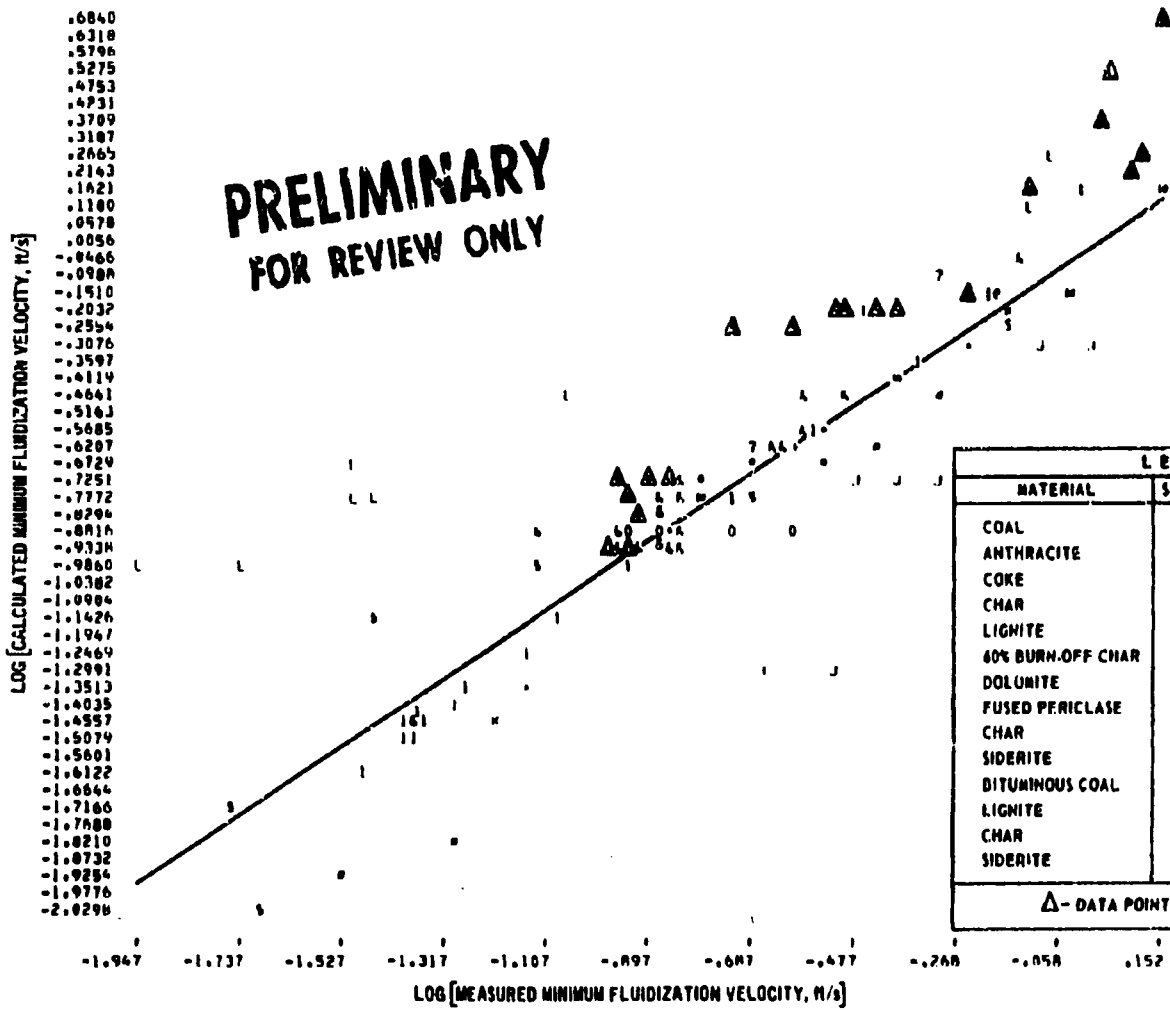
Even though Frantz's⁸ correlation compares well with data for $Re_p < 20$, it is apparent from Figure 7 that most of the measured values for $Re_p > 20$ do not show good agreement with calculated values. Because Frantz's⁸ correlation is shown in the Appendix to be good only for $Re_p < 20$, this discrepancy is not unexpected. However, if the coefficient in Wen and Yu's²⁴ correlation

Table 3. SOURCES OF FLUIDIZATION DATA FOR COALS AND RELATED MATERIALS

Investigators	Bed Diameter, inches	Fluidized Solids	Particle Diameter, inches	Particle Density, lb/cu ft	Incipient Fluidized-Bed Voidage	Shape Factor	Fluidizing Medium	Operating Temperature, °F	Operating Pressure, psig
Agarwal and Storow ¹	1.64	Coal	0.0124-0.022	82-83	Reported as porosity of settled bed	0.67	Air	70-80	0
Leva et al. ¹⁶	4.0	Anthracite	0.002-0.04	122-123	Reported	0.625 ^a	He, air	70-80	0
van Heerden et al. ²³	3.35	Coke	0.0037-0.026	112	Reported as porosity of settled bed	0.625 ^a	H ₂ , air, CO ₂ , Ar	70-80	0
Jones et al. ¹¹	3	Coal, char	0.0055-0.0189	71-80	Reported as porosity of settled bed	0.625 ^a	N ₂	70-80	2-5
Curran and Gorin ⁵	1.2	Lignite, char, dolomite, periclase	0.0028-0.0173	51-122	Calculated from bed expansion data	Included in the reported average particle diameter	N ₂ , H ₂ , CO ₂	70-80	0
Feldmann et al. ⁷	3.69	Char	0.0052-0.113	16-23	Calculated from settled bed height	0.625 ^a	CO ₂	70-80	0
Tarman et al. ²²	2.5	Siderite	0.0048-0.0084	245	Reported	0.74	Air, CO ₂ , H ₂ , Freon	70-80	0-100
Knowlton ¹²	11.5	Coal, char, lignite, siderite	0.0096-0.0113	73-245	Calculated from bed expansion data	For coals from Figure 7 and siderite from Tarman et al.	N ₂	70-80	0-1000

* Estimated.

B75030513



**PRELIMINARY
FOR REVIEW ONLY**

LEGEND		
MATERIAL	SYMBOL	REFERENCE
COAL	?	AGARWAL AND STORROW ¹
ANTHRACITE	L	LEVA <i>et al.</i> ¹⁴
COKE	I	VAN HEERDEN <i>et al.</i> ²³
CHAR	J	JONES <i>et al.</i> ¹¹
LIGHTITE	+	CURRAN AND GORIN ⁵
60% BURN-OFF CHAR	S	CURRAN AND GORIN ⁵
DOLUMITE	⊙	CURRAN AND GORIN ⁵
FUSED PERICLASE	K	CURRAN AND GORIN ⁵
CHAR	#	FELDMANN <i>et al.</i> ⁷
SIDERITE	&	TARMAN <i>et al.</i> ²²
BITUMINOUS COAL	•	KNOWLTON ¹²
LIGHTITE	Y	KNOWLTON ¹²
CHAR	0	KNOWLTON ¹²
SIDERITE	S	KNOWLTON ¹²

Δ - DATA POINTS CORRESPONDING TO $R_{0p} > 70$

B75030443

Figure 7. COMPARISON OF FRANTZ'S CORRELATION WITH MEASURED MINIMUM FLUIDIZATION DATA



EDRA
PAGE
REVISION NO.
DATE



EDRA _____
 PAGE _____
 REVISION No. _____
 DATE _____

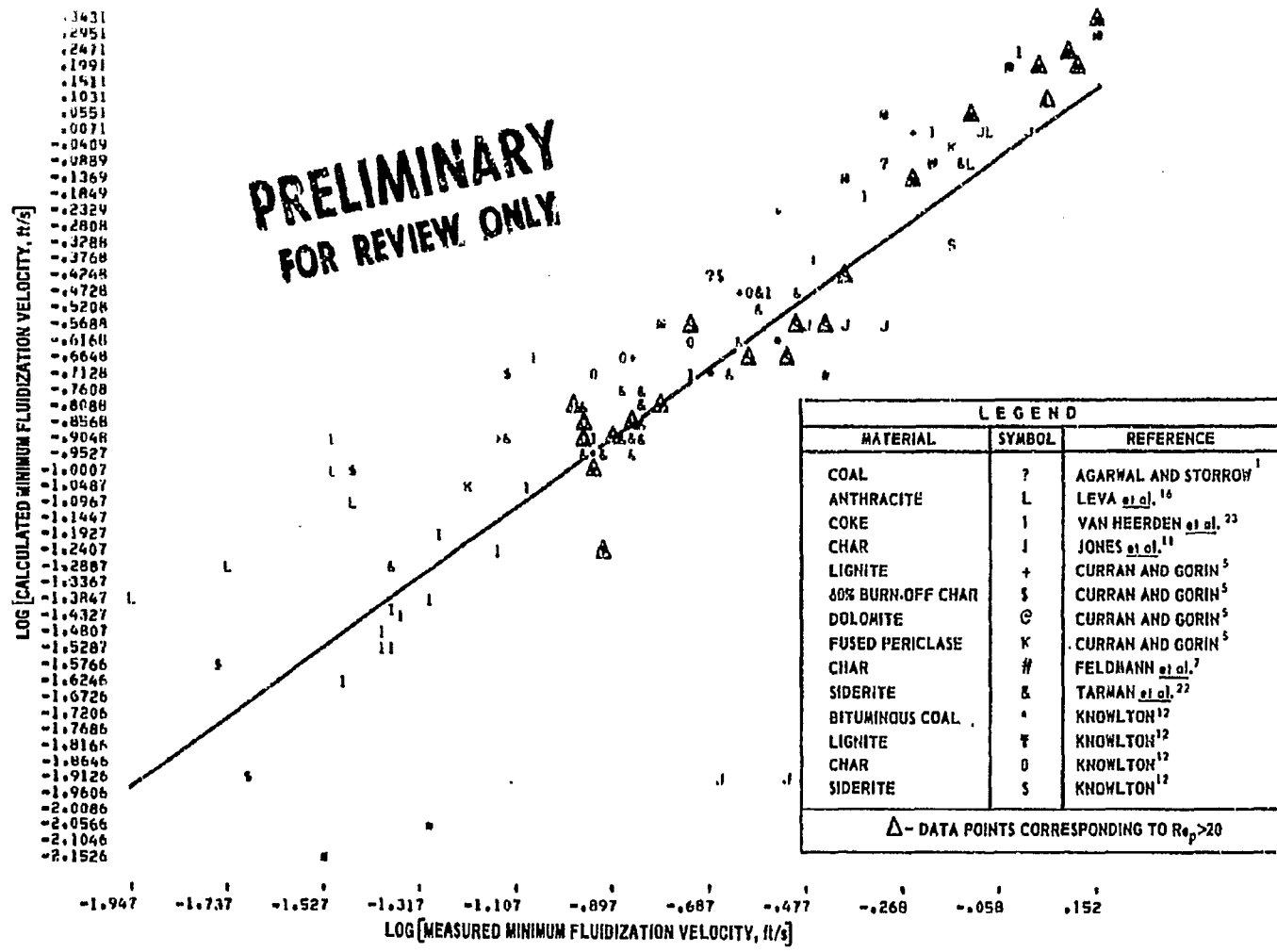


Figure 8. COMPARISON OF KUNIL-LEVENSPIEL'S CORRELATION WITH MEASURED FLUIDIZATION DATA

B75030422



EDRA
PAGE
REVISION No.
DATE

39

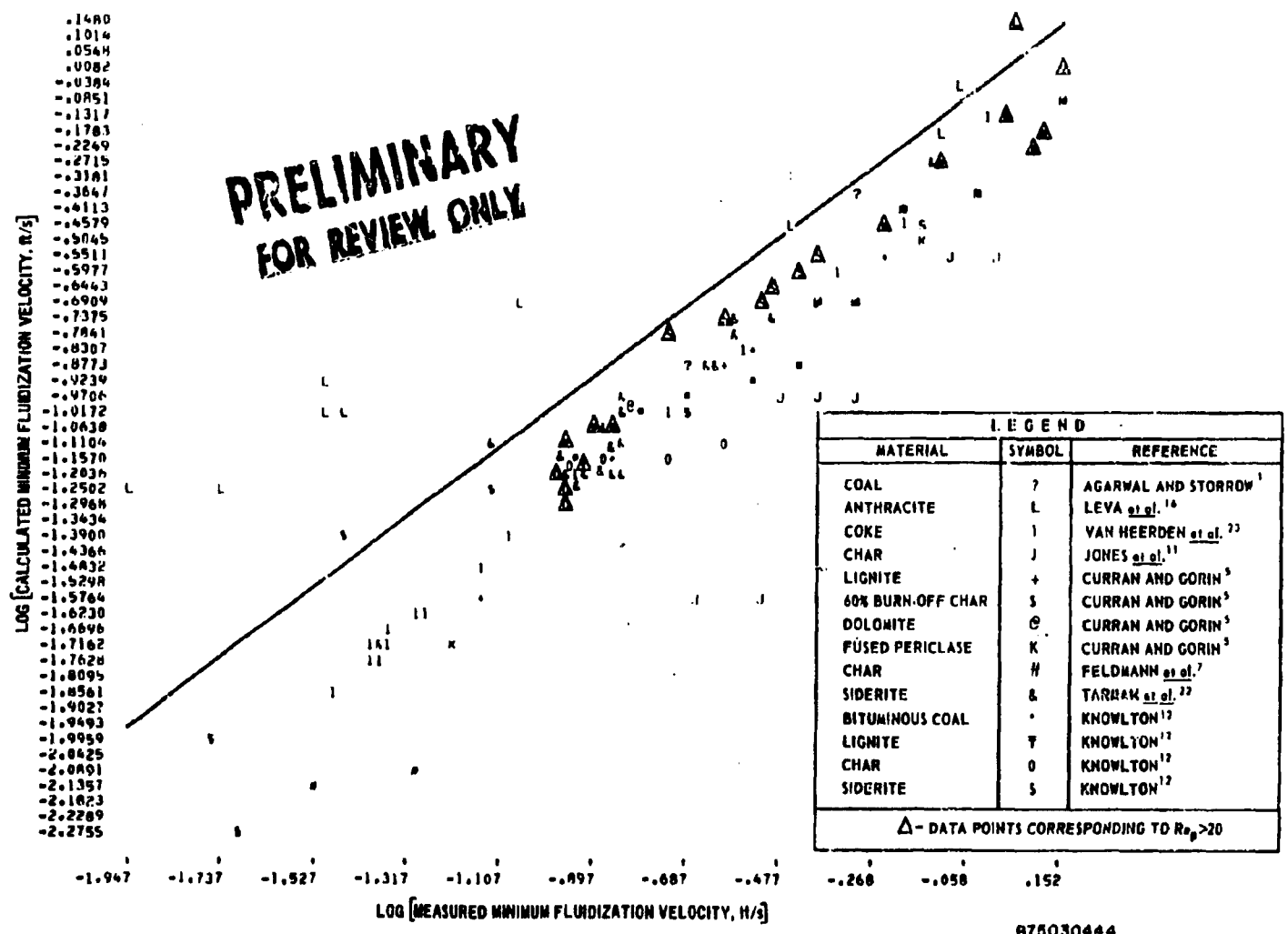
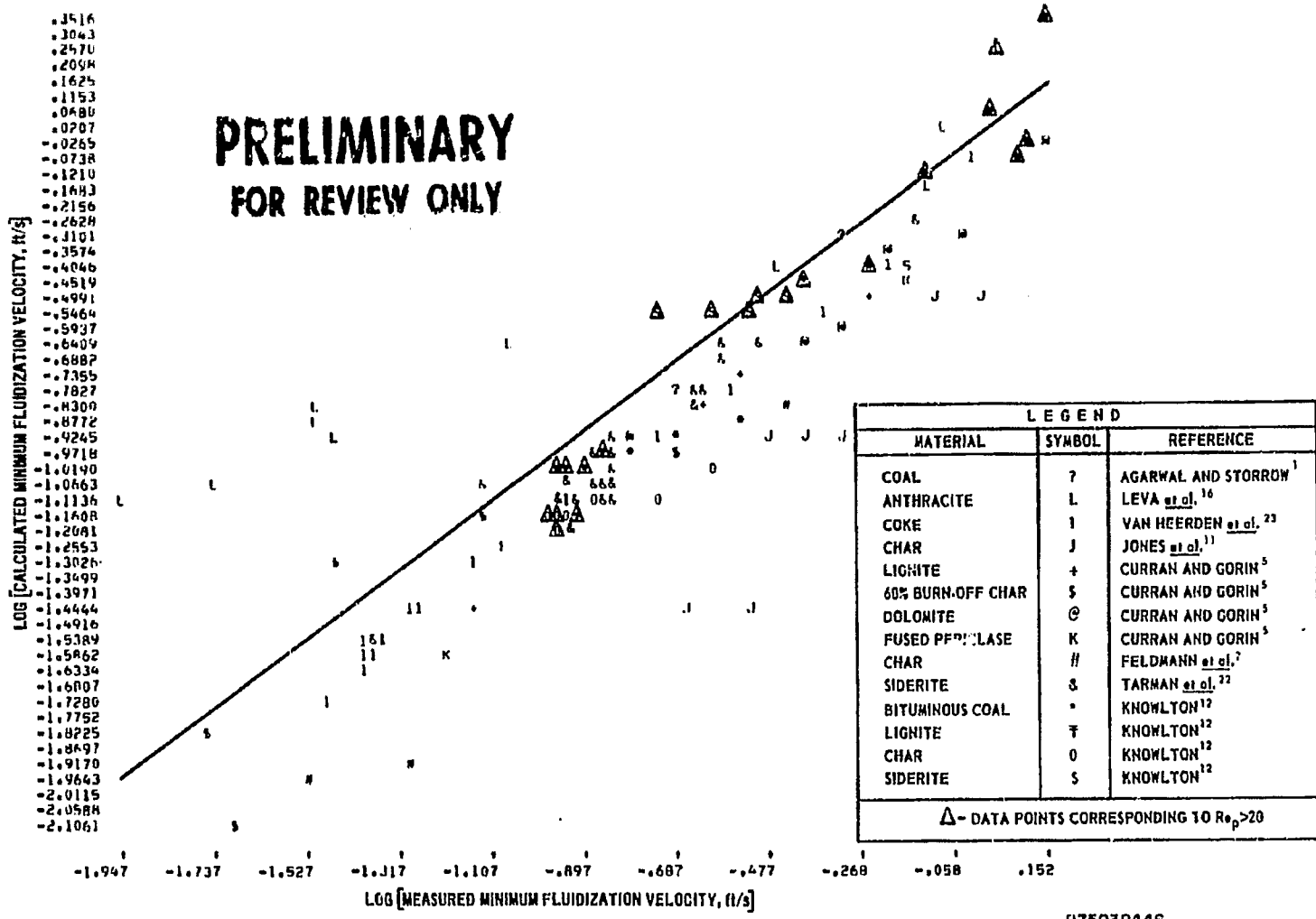


Figure 9. COMPARISON OF W_LN-YU'S CORRELATION WITH MEASURED FLUIDIZATION DATA



EDRA _____
 PAGE _____
 REVISION No. _____
 DATE _____

**PRELIMINARY
 FOR REVIEW ONLY**



LEGEND		
MATERIAL	SYMBOL	REFERENCE
COAL	?	AGARWAL AND STORROW ¹
ANTHRACITE	L	LEVA <i>et al.</i> ¹⁶
COKE	1	VAN HEERDEN <i>et al.</i> ²³
CHAR	J	JONES <i>et al.</i> ¹¹
LIGNITE	+	CURRAN AND GORIN ⁵
60% BURN-OFF CHAR	\$	CURRAN AND GORIN ⁵
DOLOMITE	@	CURRAN AND GORIN ⁵
FUSED PPT. GLASS	K	CURRAN AND GORIN ⁵
CHAR	#	FELDMANN <i>et al.</i> ⁷
SIDERITE	&	TARMAN <i>et al.</i> ²²
BITUMINOUS COAL	*	KNOWLTON ¹²
LIGNITE	7	KNOWLTON ¹²
CHAR	0	KNOWLTON ¹²
SIDERITE	S	KNOWLTON ¹²

△ - DATA POINTS CORRESPONDING TO $Re_p > 20$

40

875030446

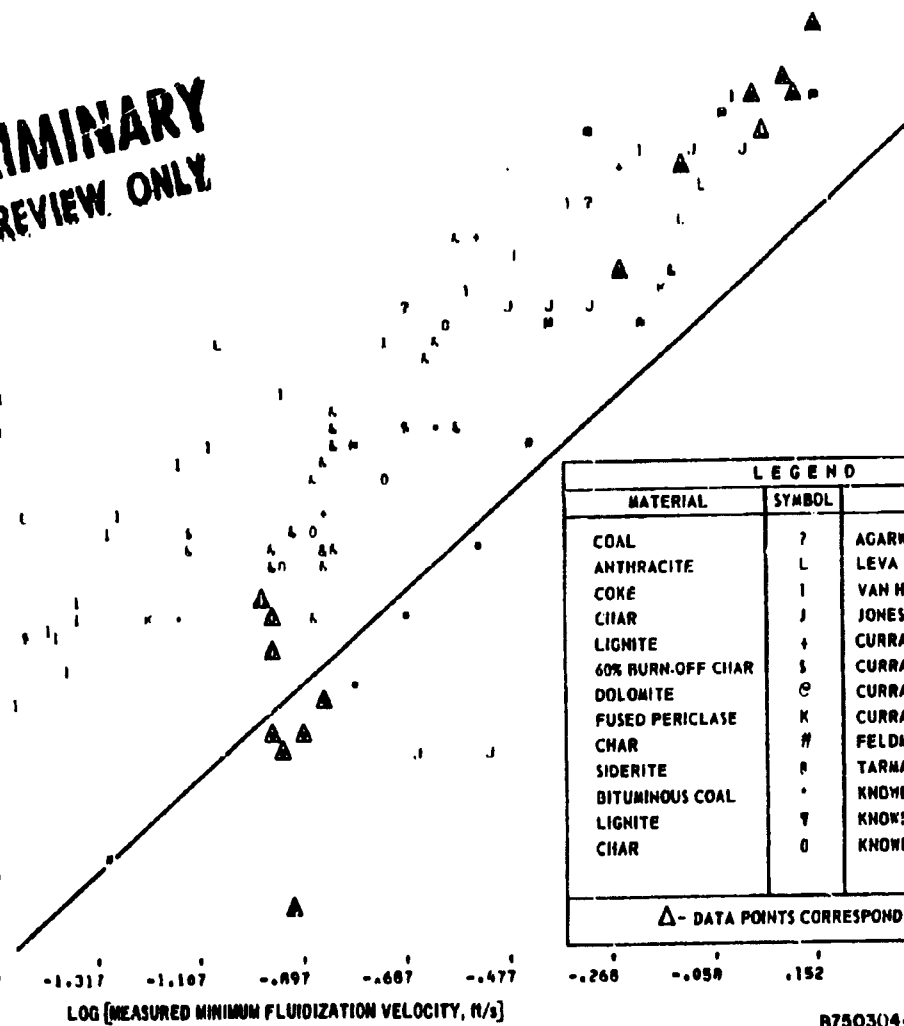
Figure 10. COMPARISON OF LEVA'S CORRELATION WITH MEASURED MINIMUM FLUIDIZATION DATA



LOG [CALCULATED MINIMUM FLUIDIZATION VELOCITY, ft/s]

0.5502
0.5119
0.4735
0.4352
0.3968
0.3585
0.3202
0.2818
0.2435
0.2051
0.1668
0.1284
0.0901
0.0517
0.0134
-0.0249
-0.0633
-0.1016
-0.1400
-0.1783
-0.2167
-0.2550
-0.2934
-0.3317
-0.3700
-0.4084
-0.4467
-0.4851
-0.5234
-0.5618
-0.6001
-0.6385
-0.6768
-0.7151
-0.7535
-0.7918
-0.8302
-0.8685
-0.9069
-0.9452
-0.9836
-1.0219
-1.0603
-1.0986
-1.1369
-1.1753
-1.2136
-1.2520
-1.2903
-1.3287
-1.3670
-1.4054
-1.4437

**PRELIMINARY
FOR REVIEW ONLY**



LEGEND		
MATERIAL	SYMBOL	REFERENCE
COAL	?	AGARWAL AND STORROW ¹
ANTHRACITE	L	LEVA <i>et al.</i> ¹⁴
COKE	I	VAN HEERDEN <i>et al.</i> ²²
CHAR	J	JONES <i>et al.</i> ¹¹
LIGNITE	+	CURRAN AND GORIN ³
60% BURN-OFF CHAR	S	CURRAN AND GORIN ³
DOLOMITE	⊙	CURRAN AND GORIN ³
FUSED PERICLASE	K	CURRAN AND GORIN ³
CHAR	#	FELDMANN <i>et al.</i> ⁷
SIDERITE	⊖	TARMAN <i>et al.</i> ²²
BITUMINOUS COAL	•	KNOWLTON ¹³
LIGNITE	∇	KNOWLTON ¹³
CHAR	0	KNOWLTON ¹³

Δ - DATA POINTS CORRESPONDING TO Re_p > 20

EDRA _____
PAGE _____
REVISION No. _____
DATE _____

41

Figure 11. COMPARISON OF ZENZ'S CORRELATION WITH MEASURED MINIMUM FLUIDIZATION DATA

B75030445

is increased to match the coefficient in Frantz's correlation,⁸ the data corresponding to $Re_p > 20$ match as well with the calculated values as do the data points for $Re_p < 20$. This improvement in comparison is conceivable because the general form of Wen and Yu's correlation, shown in Table 2, covers the entire range of Re_p .

The Kunii and Levenspiel¹⁴ correlation, derived more rigorously when compared with other correlations, covers the entire range of Re_p values. The calculated values in Figure 8 are obtained by solving the quadratic equation shown in Table 2. Unlike Frantz's correlation,⁸ the Kunii and Levenspiel correlation¹⁴ shows good agreement even with most of the measured values for $Re_p > 20$.

The graphical correlation by Zenz,²⁶ shown in Figure A-1, is developed for particulate fluidization of mostly spherical particles and materials like glass beads, cracking catalysts, and bauxite. The bed voidage at incipient fluidization conditions is critical in employing this correlation to calculate the minimum fluidization velocity. The usual lack of such data, as shown in Table 3, combined with the difficulty of using a graphical procedure makes it hard to calculate minimum fluidization velocities within a narrow range of precision. Figure 11 shows that, in general, the calculated values are up to 3 times or more greater than the measured values. This deviation is attributed to the nonavailability of accurately measured bed voidages at incipient fluidization and the difference in behavior of gas-solid fluidized beds from particulate fluidization.

The empirical correlations shown in Table 2 can be broadly divided into two categories. The first set of equations requires information on the density and viscosity of the fluidizing medium and the density and average diameter of fluidized solids. The second set of correlation needs additional information on the shape factor and the incipiently fluidized-bed voidage to estimate the minimum fluidization velocity. Thus, Frantz,⁸ Wen and Yu,²⁴ and Leva's¹⁵ correlations belong to the first set while Kunii and Levenspiel¹⁴ and Zenz's²⁶ correlations belong to the second category.

2. Evaluation of Minimum Fluidization Velocity Data

As seen in the Appendix, the general form of the published correlations to estimate the minimum fluidization velocity can be written as -

$$U_{mf} = \frac{K \cdot D_p^2 (\rho_s - \rho_g) g}{\mu} \quad (A-6)$$

U_{mf} is sensitive to the average particle diameter D_p . In coal processing, a wide size distribution of particles is frequently encountered, and therefore it is important to calculate an appropriate average diameter. Of the different types of average diameters, ^{4, 17, 20} Kunii and Levenspiel¹⁴ recommend the use of a mean particle diameter characteristic of the specific surface area of the material. By fundamental derivation, they calculate the surface mean particle diameter as -

$$D_p = \frac{1}{\sum_i \frac{X_i}{D_{pi}}} \quad (10)$$

Most of the data used to verify the models, as shown in the Appendix, report average particle diameters defined by Equation 10, except for Leva et al.,¹⁶ who calculated a mean diameter using -

$$\bar{d}_p = \sum_i X_i \cdot d_{pi} \quad (11)$$

For a given size distribution, \bar{d}_p is greater than D_p , and, as a result, the calculated minimum fluidization velocities for anthracite coal reported by Leva et al.¹⁶ are significantly higher than the measured values as shown in Figures 7 through 11. It is apparent that, if the average particle diameters for these data are recalculated using Equation 10, the comparison between the calculated and measured minimum fluidization velocities will be improved.

To estimate the minimum fluidization velocity, the particle density of the fluidizing solids must be accurately determined while the density of the fluidizing medium is not critical for low-pressure operations. Nevertheless, in high-pressure fluidization, the correct density of the fluidizing medium should be used.

A precise estimation of the viscosity of the fluidizing medium is essential to calculate the minimum fluidization velocity. In general, the effect of temperature is much more significant on viscosity than pressure. Because coal processing involves fluidization with mixtures of gases, at high temperatures (up to 2000°F) and high pressures (up to 1250 psig), a reliable method of estimating viscosity must be used.

In Figures 7 through 10 we see that the calculated values using the tested correlations differ significantly from the measured values reported by Feldmann et al.⁷ This is attributed to the method by which these investigators estimate particle density from particle size. The fact that the particle density decreases abruptly at a particle diameter of about 0.005 in. with decreasing particle size may be unique to the chars used by these investigators. The possibility of the interlocking of char particles during fluidization, envisioned by Feldmann et al.,⁷ could very well be an additional factor in explaining the deviation of the calculated values from the measured values. However, measured values of particle densities of representative samples and an appropriate estimate of an average particle diameter could result in better agreement between the correlations and the data.

The COED char fluidization data by Jones et al.¹¹ show consistently lower calculated values in Figures 7 through 10. The important reasons for this discrepancy include the segregation of particles by size and the effect of bed height encountered by these investigators. The segregation of particles presented a difficulty to Jones et al.¹¹ when they measured the point of incipient fluidization. Working with increasing bed heights, they reported mostly increasing minimum fluidization velocity values, which cannot be predicted by the available correlations. Compounding these problems is the possibility that the coefficients in the tested correlations may be inadequate in describing the fluidization system that Jones et al.¹¹ used.

A problem similar to the varying bed heights is encountered in verifying the models for minimum fluidization with the high-pressure fluidization data from Tammann et al.²² and Knowlton.¹² The tested correlations, being developed from atmospheric fluidization data, have no provision to adequately describe fluidized beds operating at higher pressures, except in terms of the density of the fluidizing medium. For example, in the experiments

conducted by Knowlton,¹² even though the fluid density changes from about 0.07 to 5 lb/cu ft, the magnitude of the term $(\rho_s - \rho_g)$ in Equation A-6* does not change significantly, in particular for dense materials like siderite. However, we see from the results of these investigators that the incipient-bed voidage decreases with an increase in operating pressure. The Kunii and Levenspiel correlation,¹⁴ which includes the incipient-bed voidage in addition to the shape factor, illustrates a better comparison with these measured values in contrast to the correlations developed by Leva,¹⁵ Frantz,⁸ and Wen and Yu.²⁴ As explained before, the calculated values for Tarman et al.²² and Knowlton's data¹² do not show any change with pressure when using the Leva,¹⁵ Frantz,⁸ and Wen and Yu²⁴ correlations. However, by including bed voidage at incipient fluidization, the Kunii and Levenspiel correlation¹⁴ calculates a decreasing minimum fluidization velocity with increasing pressure, which is in agreement with the reported experimental data. From Figure 8 it is apparent that with the later correlation most of the calculated values using Tarman's²² and Knowlton's¹² data are within $\pm 10\%$ of the measured minimum fluidization velocities.

In the present investigation, the shape factor, even when it was not available, was determined from Figure 12, using the proximate analysis of coal.² Whenever the proximate analysis was not reported, a value of 0.625 was assigned.¹⁶ The incipient fluidized-bed voidage was calculated from the reported particle and bulk densities, when such data were unavailable. This method of calculating minimum bed voidage is known to result in values less than the incipient fluidized-bed voidage. Therefore, the inherent deficiencies with such sources of data must be recognized in comparing them with the Kunii and Levenspiel correlation,¹⁴ which is sensitive to shape factor and the bed voidage at the onset of fluidization.

In Figure 8, the Leva et al., data¹⁶ on anthracite show the usual higher calculated values, and the data by Jones et al.,¹¹ with inadequate information for using the Kunii and Levenspiel correlation,¹⁴ result in minimum fluidization velocities significantly different from the measured values. The data reported by Feldmann et al.,⁷ do not include information on shape factors.

* See the Appendix.

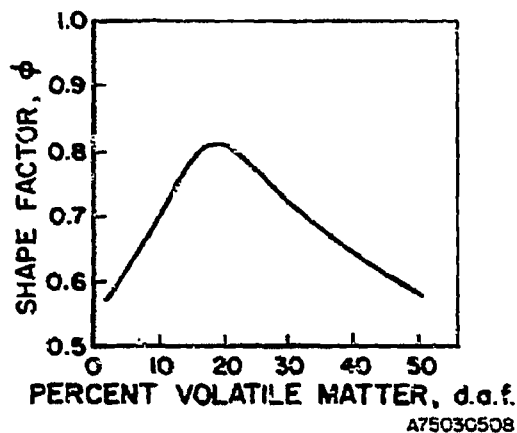


Figure 12. RELATION BETWEEN SHAPE FACTOR, ϕ , AND PERCENTAGE VOLATILE MATTER (d.a.f.) OF COAL ²

However, the combination of the assumed value of the shape factor and the method described earlier to determine the particle density has resulted in calculated values, using the Kunii and Levenspiel correlation,¹⁴ to be in fairly good agreement with the measured values as shown in Figure 8, except for the two points at very low minimum fluidization velocities.

The experimental data on coke reported by van Heerden²³ contain most of the required information and shows excellent agreement with the Kunii and Levenspiel correlation¹⁴ as shown in Figure 8.

The calculated minimum fluidization velocities using the Frantz⁶ and the Kunii and Levenspiel¹⁴ correlations are up to about 50% greater than the measured data reported by Curran and Gorin⁵ for materials of different density. The calculated values show better agreement with the lighter materials like lignite char and 60% carbon burn-off char compared with heavier materials like dolomite and periclase. It is conceivable that either the physical properties of these solids or the empirical coefficients in the tested correlations are not adequately descriptive of the dense materials.

Based on this extensive discussion comparing the published correlations with measured minimum fluidization data, for coal and related materials, specific recommendations will be proposed in subsequent monthly reports.

Nomenclature

- B = generalized shape factor
- D_{av} = harmonic mean diameter of mixture, ft
- D_f = particle diameter of a sieved fraction, ft
- D_p = average particle diameter, ft = $\frac{1}{\sum (X/D_f)}$
- g = gravitational constant, ft/s²
- Re_p = particle Reynold's number = $(D_p \cdot U_{mf} \cdot \rho_g / \mu)$
- U_{mf} = minimum fluidization velocity, ft/s
- U_t = terminal velocity, ft/s
- X = weight fraction of sieved particles
- ϵ_{mf} = voidage of minimum fluidized bed
- ϕ = shape factor
- ρ_g = density of fluidizing gas, lb/CF
- ρ_s = particle density of fluidizing solids, lb/cu ft
- ρ_B = settled bed density, lb/cu ft
- $\rho_{s_{av}}$ = arithmetic average density of mixture, lb/cu ft
- ρ_{Bm} = bed density at maximum porosity, lb/cu ft
- μ = viscosity of fluidizing gas, lb/ft-s

References Cited

1. Agarwal, O. P. and Storrow, J. A., "Pressure Drop in Fluidized Beds - Part I," Chem. Ind. (London), 278-86 (1951) April 14.
2. Austin, L. G., Gardner, R. P. and Walker, P. L., Jr., "The Shape Factors of Coals Ground in a Standard Hardgrove Mill," Fuel **42**, 319 (1963) July.
3. Baerg, A., Klassen, J. and Gisher, P. E., "Heat Transfer in a Fluidized Solids Bed," Can. J. Res. **F28**, 287 (1950).
4. Coulson, J. M. and Richardson, J. F., Chemical Engineering, Vol. **2**, 488-92. London: Pergamon Press, 1962.
5. Curran, G. P. and Gorin, E., "Studies on Mechanics of Fluo-Solids Systems," prepared for Office of Coal Research, Contract No. 14-01-0001-415, Interim Report No. 8, Book 1. Washington, D. C., 1970.
6. Davies, L. and Richardson, J. W., "Gas Interchange Between Bubbles and the Continuous Phase in a Fluidized Bed," Trans. Inst. Chem. Eng. **44**, 293 (1966).
7. Feldmann, H. F., Kiang, K. and Yavorsky, P., "Fluidization Properties of Coal Char," Symposium on Gasification of Coal, 162nd National Meeting, ACS Division of Fuel Chemistry Preprints **15**, (3), 62-76 (1971) September.
8. Frantz, J. F., "Minimum Fluidization Velocities and Pressure Drop in Fluidized Beds," Chem. Eng. Progr. Symp. Ser. **62**, 21-31 (1966).
9. Goroshko, V. D., Rozenbaum, R. B. and Todes, O. M., "Approximate Hydraulic Relationships for Suspended Beds and Hindered Fall," Izvestiya VUZov, Neft i Gaz, No. **1**, 125-31 (1958).
10. Johnson, E. "Institute of Gas Engineers Report," Publication No. 318/179, London, 1949-50.
11. Jones, J. F., Eddinger, R. T. and Seglin, L., "Pyrolysis of Agglomerating Coals in Multiple Fluidized-Bed Reactors," in Proceedings of the International Symposium on Fluidization. Amsterdam: Netherlands Univ. Press, 1967.
12. Knowlton, T. M., "High-Pressure Fluidization Characteristics of Several Particulate Solids: Primarily Coal and Coal-Derived Materials." Paper No. 9b, presented at the 67th Annual Meeting of the A. I. Ch. E., Washington, D. C., December 1-5, 1974.
13. Kumar, A. and Sen Gupta, P., "Prediction of Minimum Fluidization Velocity for Multicomponent Mixtures (Short Communication)," Indian J. Technol. **12**, No. 5, 225 (1974).
14. Kumii, D. and Levenspiel, O., Fluidization Engineering. New York: John Wiley, 1969.
15. Leva, M., Fluidization. New York: McGraw-Hill, 1959.
16. Leva, M., Weintraub, M., Grummer, M. and Polichik, M., "Fluidization of an Anthracite Coal," Ind. Eng. Chem. **41**, 1206 (1949).

17. McCabe, W. L. and Smith J. C., Unit Operations of Chemical Engineering, 2nd Ed., 792-98. New York: McGraw-Hill, 1967.
18. Miller, C. O., and Logwinuk, A. K., "Fluidization Studies of Solid Particles," Ind. Eng. Chem. **43**, 1220 (1951).
19. Narasimhan, G., "On a Generalized Expression for Prediction of Minimum Fluidization Velocity," A.I.Ch.E. J. **11**, 550 (1965).
20. Orr, C., Jr., "Size Measurement of Particles," Encyclopedia of Chemical Technology, Supplementary Volume. New York: McGraw-Hill, 1959.
21. Pillai, B. C. and Raja Rao, M., "Pressure Drop and Minimum Fluidization Velocities in Air-Fluidized Beds," Indian J. Technol. **9**, 77-86 (1971) March.
22. Tarman, P., Punwani, D., Bush, M. and Talwalkar, A., "Development of the Steam-Iron System for Production of Hydrogen for the HYGAS Process," prepared for Office of Coal Research, Contract No. 14-32-0001-1518, R&D Report No. 95, Interim Report No. 1. Washington, D. C., 1974.
23. van Heerden, C., Nobel, A. P. P. and van Krevelen, D. W., "Studies on Fluidization I - The Critical Mass Velocity," Chem. Eng. Sci. **1**, No. 1, 37-49 (1951).
24. Wen, C. Y. and Yu, Y. H., "Mechanics of Fluidization," Chem. Eng. Progr. Symp. Ser. **62**, 100-11 (1966).
25. Wilhelm R. H. and Kwauk, M., "Fluidization of Solid Particles." Chem. Eng. Progr. **44**, 20 (1948).
26. Zenz, F. A., "Calculate Fluidization Rates," Pet. Refiner **36**, No. 8, 147-55 (1957).

Errata

In last month's report (Project 8964 January 1975 Status Report) the following corrections are to be noted:

1. In Table 2, Zenz's graphical correlation was mentioned but not included in the report. This is the same correlation given in the Appendix in this month's report (Figure A-1).
2. In Table 3, the fluidizing medium for the data of Jones et al., should be changed from "CO + H₂, steam" to "N₂."
3. In Table 3, the particle diameter range for van Heerden et al.'s data should read "0.0037-0.026 inch."
4. In Table 3, the particle diameter range for Tarman et al.'s data should be "0.0048-0.0084" instead of "0.0048 to 0.0053" as reported.

D. COMBUSTION

A meeting is planned with Gilbert Associates to discuss this section of the data book.

Errata

In last month's report (Project 8964 January 1975 Status Report), the particle diameter limit for Equation 4 should read " $d_p \geq 1.5 \text{ mm}$ " instead of " $d_p \leq 1.5 \text{ mm}$."

E. COAL, CHAR, AND OIL SHALE PROPERTIES

1. Data Compilation

We conferred with Professor W. Spackman and his associates involved in work on coal properties at Pennsylvania State University. Our proposed use of Penn State's data for a compilation of properties of selected coal samples (Table 2 in the Project 8964 December 1974 Status Report) was the main topic of consideration.

Penn State people suggested that we include the free-swelling index and ash-fusibility data in the compilation. Channel and run-of-mine samples representing large deposits capable of sustaining a coal conversion plant will be selected from Penn State's PSOC series for inclusion in the compilation. These data will be augmented by additional information from other sources such as U. S. and state geological surveys and the Bureau of Mines. Penn State will endeavor to fill in the missing gaps in these data to complete the compilation table by including these samples in its PSOC series.

Penn State is in the process of verifying its computer record of data on its present set of samples. It expects to give us data on samples representing the 50 largest deposits of its set as soon as possible. We have also begun to compile a list of large ($\sim 10^9$ tons) coal deposits in the United States to compare with the Penn State list. This list, prepared from an early 1950's study, is given in Table 4.

A schedule of proposed data transmittal, current and future, has been requested from Penn State.

Table 4. COAL DEPOSITS IN THE UNITED STATES*

<u>State</u>	<u>County</u>	<u>Rank</u>	<u>Reserves Recoverable, ~ 10⁹ (billion) tons</u>
Colorado	Northwest Gunnison	lvCb	1.859089
	Central Las Animas	lvAb	1.969641
	Delta	SubA	0.963276
	Moffat-Rio Blanco	lvCb	2.347832
	Routt	lvCb	1.510974
Illinois	Perry	lvBb-lvCb	1.022846
	Saline	lvAb-lvBb	0.801624
	Northern Christian	lvCb	0.899764
	Macoupin	lvCb	1.866784
	Southeastern Montgomery	lvCb	1.220676
	St. Clair	lvCb	0.919120
	Sangamon	lvCb	1.612940
Indiana	Gibson-Fike	lvBb	1.370877
	Sullivan	lvCb	2.084892
	Vanderburgh- Warrick	lvCb	1.258032
Kentucky	Muhlenberg-Mclean	lvBb	1.039476
	Hopkins-Christian	lvBb	1.401016
	Webster	lvAb-lvBb	0.784986
	Pike	lvAb	2.560579
	Harlan-Letcher	lvAb	1.089054
	Floyd-Magoffin	lvAb	1.060825
Montana	Musselshell- Yellowstone	SubA-SubB	1.261249
	Central Rosebud	SubB-SubC	1.870758
	Southwestern Custer	SubB-SubC	1.307768
	Richland-Dawson- Wibaux	Lignite	0.829638
	Rosebud-Bighorn	SubB-SubC	0.997090
	Powder River	SubC-Lignite	1.958616
	Southeastern Bighorn	SubC	1.550324
	Southern Rosebud Bighorn	SubC	1.922334
	Treasure-Bighorn	SubB-SubC	1.020724

Table 4. Cont. COAL DEPOSITS IN THE UNITED STATES*

<u>State</u>	<u>County</u>	<u>Rank</u>	<u>Reserves Recoverable, ~ 10⁹ (billion) tons</u>
North and South Dakota	Billings, Stark, Dunn, Slope, Bowman	Lignite	1.244182
	Williams	Lignite	0.751758
Ohio	Belmont	hvAb	1.572850
Pennsylvania (Bituminous)	Washington	hvAb	1.481944
	Cambria	lvb-mvb	1.386676
	Eastern Armstrong	hvAb	0.764262
	Southwestern Indiana	hvAb	0.755928
Utah	Central Carbon	hvAb-hvCb	0.795804
West Virginia	Raleigh	lvb-mvb	0.998207
	Wyoming		0.805674
	Mcdowell	lvb-mvb	1.207312
	South Kanawha	hvAb	0.870370
	Fayette		
	Logan-Wyoming	hvAb	1.458191
	Boone-Raleigh	mvb-hvAb	1.448090
Wyoming	Central Sweetwater	hvCb	0.884296

* Source: Ford, Bacon & Davis, Inc., "The Synthetic Liquid Potential of the United States," Summary Report for Bureau of Mines, Department of the Interior. New York, March 3, 1952.

Other properties of coal than those selected for compilation were also discussed briefly. Penn State is obtaining information on the mineral matter in its PSOC series. Studies on 57 coal samples have already been published — OCR Research and Development Report No. 61, Interim Report No. 2. Eight major elements and 22 trace elements were determined in these samples. In addition, semiquantitative mineralogical analyses were reported.

Dr. Frank Vastola furnished information on the Penn State computer bank of literature on carbon and associated materials. Literature on coal, starting with 1973 and 1974, is being added to the bank and is expected to be ready in April. We have requested bibliographical information on gasification reactivity, specific heat, and thermal conductivity of coal, coke, and char from this service.

We discussed the type of char data that can be included in the data book with Dr. Phil Walker. He pointed out the difficulties involved in obtaining general char data since char properties depend on the history of char. This includes method of preparation, temperature, atmosphere, and residence time of the process, as well as the starting material. The possibility of including properties of "standard" chars produced in various conversion processes was discussed. This may also prove to be difficult because the operating parameters required to characterize the char may not be available.

2. Heats of Combustion of Chars

In the course of analyzing chars obtained from the different stages of HYGAS[®] operation, we have the ultimate analyses and heats of combustion for 124 samples of chars from a single lignite source. The composition ranges of the chars and the average composition of the original coal are as follows:

	<u>Char(Range)</u>	wt %	<u>Original Coal (Avg)</u>
Ash	13-51		11.6
C	46-78		61.3
H	0.4-4		3.7
S	0.05-1.1		1.0
N	0.2-1.3		1.0
O (by difference)	1.5-13		36
C (conversion)	10-85		0
Heat of Combustion, Btu/lb	6,800-12,800		10,000

The calculation of the heat of combustion from the char composition is necessary in the design of coal gasification systems. Therefore, the accuracy of some correlations that have been used for coals was tested with these chars. The four expressions used were as follows:

Mott and Spooner¹

$$H_c = 144.54 C + 610.2 H + 40.5 S - 62.5 O$$

Dulong¹

$$H_c = 145.44 C + 620.28 H + 40.5 S - 77.54 O$$

Boie²

$$H_c = 151.2 C + 499.8 H + 45.0 S + 27 N - 47.7 O$$

Grummel and Davies¹

$$H_c = [654.3 H / (100 - \text{ash}) + 424.62] (C/3 + H - O/3 + S/8)$$

In the above, H_c is the gross heat of combustion in Btu/lb, and the composition is expressed in weight percent. In the following table, the accuracy of these correlations when applied to lignite chars, are compared.

	<u>Average Deviation, Btu/lb</u>	<u>Correction Term</u>	<u>Standard Deviation After Correction</u>
Mott and Spooner ¹	113	-70	79
Dulong ¹	127	-59	101
Boie ²	362	-362	88
Grummel and Davies ¹	84	+23	80

Used as is, that of Grummel and Davies¹ has the lowest average deviation. In the others, consistent deviations account for a significant portion of the observed deviations. The correction terms indicated, if applied to the calculated value, make the uncertainty of the other correlations comparable with that of Grummel and Davies¹ as shown in the standard deviations.

Simple modification of any of the above correlations by the addition of linear composition terms (such as changes in the coefficients of the above correlations) results in expressions with a standard deviation of about 70 Btu/lb. Other modifications are being evaluated for a more significant improvement in accuracy. The contribution of the uncertainty in the ultimate

analysis toward limiting the accuracy of these correlations is also being examined.

References Cited

1. Selvig, W. A. and Gibson, F. H., "Calorific Value of Coal," in Lowry, H. H., Ed., Chemistry of Coal Utilization, Vol. 1, 139. New York: John Wiley, 1945.
2. van Krevelen, D. W., Coal, 416. Amsterdam: Elsevier, 1961.

F. MISCELLANEOUS

Letters were sent out to various people involved in gasification studies for kinetic or other data that they may have that could be included in the data book. A sample of presentation of IGT data was also included as an example.

A list of persons contacted and the responses received so far are given in Table 5.

IV. Patent Status

The work performed during February is not considered patentable.

V. Future Work

Data collection and correlation will be continued in the selected high-priority areas.

We will meet in March with Gilbert Associates (concerning fluidized-bed combustion, low-Btu gasification, and MHD), the Bureau of Mines in Pittsburgh, Ralph M. Parsons Co., and Fluor Engineers and Constructors, Inc. (concerning liquefaction) to get their inputs in their respective areas of expertise.

Approved W. W. Bodle
W. W. Bodle, Director
Process Analysis

Signed A. Talwalkar
A. Talwalkar, Coordinator,
Process Data

Table 5. LIST OF PEOPLE CONTACTED
INVOLVED IN GASIFICATION STUDY

<u>Name</u>	<u>Company</u>	<u>Response</u>
Mr. Bob Grace	Bituminous Coal Research, Inc.	Agreed to a suggested discussion meeting
Mr. A. J. Forney	U.S. Department of the Interior	Work in gasification kinetics area not progressed sufficiently for data book presentation
Mr. R. J. Belt	Morgantown Energy Research Center	
Mr. George Curran	CONOCO Coal Development Company	
Dr. Alan Sass	Garrett Research & Development Company	
Dr. J. F. Jones	FMC Corporation	
Dr. R. Tracy Eddinger	FMC Corporation	
Dr. W. M. Goldberger	Battelle Memorial Institute	Data not available in suitable form
Dr. George T. Skaperdas	The M. W. Kellogg Company	Referred to <u>OCR Research and Development Report No. 38</u> . Subsequent work not available for dissemination
Mr. Frank Cannon	Koppers Co., Inc.	
Mr. Ronald J. McGarvey	Applied Technology Corporation	
Mr. Dennis Eastland	Davy Power Gas	IGT letter forwarded to Lakeland office for comments
Mr. Richard J. Rutherford	Riley Stoker Corporation	
Mr. Paul Rudolph	Lurgi Mineraloitechnik, GmbH	

APPENDIX. Comparison of Some Published Correlations for
Calculating Minimum Fluidization Velocities

The generally used correlations to calculate minimum fluidization velocity* are simplified and summarized below:

Leva's Correlation:¹⁵

$$U_{mf} = 0.0088 \frac{D_p^{1.22} (\rho_s - \rho_g)^{0.44} g}{\rho_g^{0.04} \mu^{0.22}} \quad (A-1)$$

Frantz's Correlation:⁸

$$U_{mf} = 0.001065 \frac{D_p^2 (\rho_s - \rho_g) g}{\mu} \quad (A-2)$$

Wen and Yu's Correlation:²⁴
(for $Re_p < 20$)

$$U_{mf} = 0.00061 \frac{D_p^2 (\rho_s - \rho_g) g}{\mu} \quad (A-3)$$

Kunii and Levenspiel's
Correlation:¹⁴
(for $Re_p < 20$)

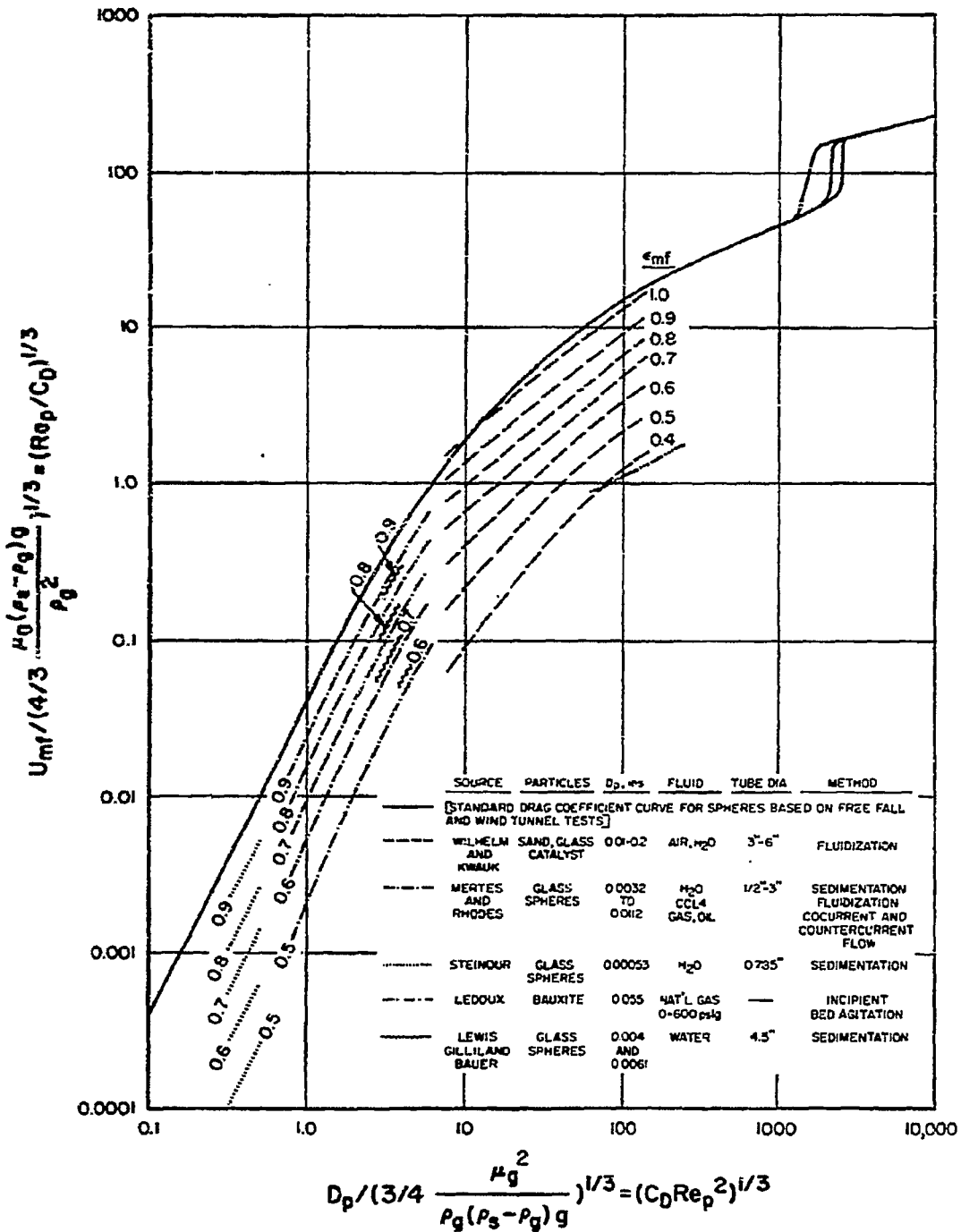
$$U_{mf} = 0.0067 \frac{e^2 \cdot \epsilon_{mf}^3}{(1 - \epsilon_{mf})} \cdot \frac{D_p^2 (\rho_s - \rho_g) g}{\mu} \quad (A-4)$$

In the graphical correlation published by Zenz,² shown in Figure A-1, the constant voidage lines up to $\log_n (C_D \cdot Re_p^2)^{1/3}$ equal to 10, can be assigned a slope of about 2.0. For this region, the relationship between the coordinates can be simplified to the following form:

$$U_{mf} = \frac{K_1 \cdot D_p^2 (\rho_s - \rho_g) g}{\mu} \quad (A-5)$$

where K_1 is a constant dependent on the fluidized-bed voidage.

* See Project 8964 January 1975 Status Report.



A7503059

Figure A-1. MODIFIED PLOT OF DRAG COEFFICIENT FOR SEDIMENTATION; FLUIDIZATION AND WIND TUNNEL TESTS OF SINGLE PARTICLES AND SUSPENSIONS ²⁶

It can be seen that Equations A-1 through A-5 are of the same general form given by -

$$U_{mf} = \frac{K \cdot D_p^2 (\rho_s - \rho_g) g}{\mu} \quad (A-6)$$

and differ by the value of their coefficients. It is conceivable that these coefficients were descriptive of the physical systems tested by individual investigators. Because Equations A-1, A-2, A-3, and A-4 match Kunii and Levenspiel's correlation for $Re_p < 20$, we can conclude that the corresponding correlations are satisfactorily descriptive of a fluidized bed up to a particle Reynold's number of 20.

[Note: References for the Appendix are listed at the end of the section, "C. FLUIDIZATION," in the main body of this report.]

IGT-MPR--5

INSTITUTE OF GAS TECHNOLOGY



3424 SOUTH STATE STREET

IT CENTER

CHICAGO, ILLINOIS 60616

AFFILIATED WITH ILLINOIS INSTITUTE OF TECHNOLOGY